TCFE10: TCS Steel and Fe-alloys Database

Database name:	TCS Steel and Fe-alloys Database	*Database acronym:*	TCFE
Database owner:	Thermo-Calc Software AB	*Database version:*	10

TCFE10 is a thermodynamic database for different kinds of steels and Fe-based alloys, such as stainless steels, high-speed steels, tool steels, high-strength low alloy (HSLA) steels, cast irons, corrosion-resistant high strength steels, low-density steels, and also cemented carbides.

It can be used together with Thermo-Calc and these specialized modules and features:

- The add-on modules: Diffusion Module (DICTRA), Precipitation Module (TC-PRISMA) and Process Metallurgy Module.
- The Steel Model Library, which includes martensite and pearlite models designed to help experts working in the steel industry to quickly and easily set up calculations using the Property Model Calculator.
- The Software Development Kits (SDKs) including TC-Python and the TQ-Interface.

The database is developed and validated for simulation of the solidification process, the relative stability of matrix phases (austenite and ferrite), precipitation of secondary phases such as sulfides, borides, oxides, phosphides, carbides, nitrides, carbonitrides, and also intermetallic phases such as the sigma and laves phases.

Scope of the Database

The TCFE10 database contains the thermodynamic descriptions for 29 elements and more than 308 binary, 269 ternary, and 77 quaternary systems. It also includes several quinary systems.

Included Elements (29)

Ar	Al	B	C	Ca	Ce	Co	Cr	Cu	Fe
H	Mg	Mn	Mo	N	Nb	Ni	O	P	Ru
S	Si	Ta	Ti	V	W	Y	Zn	Zr	

The TCFE10 database is applicable for various types of steels/Fe-alloys with an Fe-minimum of 50 wt.%. For alloying elements, the recommended composition limits are given in the table below.

Table 2. The recommended composition limits (wt.%) in the TCFE10 database.

Element	Max	Element	Max	Element	Max	Element	Max
Al	10	Cu	5	O	Trace	V	15.0
B	Trace	Mg	Trace	P	Trace	W	15
C	7	Mn	30	Ru	15	Y	*
Ca	Trace	Mo	10	S	Trace	Zn	**
Ce	Trace	N	5	Si	5	Zr	10
Co	20	Nb	5	Ta	10.0		
Cr	30	Ni	20	Ti	3.0		

*Y systems are included mainly for the purpose of oxide dispersion strengthened (ODS) steels with many assessed oxygen containing binary and ternary systems within the Al-Cr-Cu-Fe-Mn-Ni-O-Si-Y-Zr frame of elements.

** The element Zn has been further treated with the focus on the Zn corner of Al-Cr-Fe-Zn system for galvanization process, but several other binaries and ternaries are also included.

Ar and H are only considered in the gas phase and no modeling of solubility in the solid solution phases or liquid is taken into account.

A sensible calculation cannot be expected if all alloying elements are at their highest limits. Some combinations of elements at high values do not give reasonable results. However, some alloying elements can exceed their limits considerably and the calculations still give good results.

The critical calculations must always be verified by equilibrium experimental data; it is your responsibility to verify the calculations.

If you discover any significant deviations and want to help us improve future versions of the database, please contact Thermo-Calc Software at one of our offices or send us an email at info@thermocalc.com.

The database is developed on the basis of complete assessments of binary, ternary, and some higher order systems. However, many intermediate compounds that usually do not occur in steels/Fe-alloys are ignored in the database. Therefore, the database may not be suitable to calculate complete binary and ternary systems, but only rather in the Fe-rich corner.

Sometimes, for some special steels/Fe-alloys, you may prefer to append some other stoichiometric or solution phases (usually intermediate compound phases that have been ignored in the *TCFE Database*) from another compatible database (e.g. *SSOL: SGTE Solutions Database* and/or *SSUB: SGTE Substances Database*). But you must be careful about appropriately appending such data in the combination.

The *TCFE* database contains an extensive GAS mixture phase (Ar and different species in the C-H-N-O-S system) for the main purpose of considering oxygen/nitrogen-gas controls in steel-making processes and different gas atmospheres under, for example, heat treatments. However, it can be replaced by an even more comprehensive description of the GAS phase appended from a compatible database e.g. *SSUB: SGTE Substances Database* or *SLAG: TCS Fe-containing Slag Database*.

Similarly, an IONIC_LIQ solution phase can be appended from the *TCOX: TCS Metal Oxide Solutions Database*, when it is really necessary to consider a more comprehensive ionic liquid phase for calculations of e.g. formations of complex oxides on steel surfaces. However, for the purposes of investigating various steelmaking metallurgical processes, it is recommended to append the so-called SLAG solution phase from e.g. *SLAG: TCS Fe-containing Slag Database*. In the meantime, keep in mind that the SLAG and IONIC_LIQ phases should never be simultaneously considered in the same defined system/calculation, as they both represent the slag mixture but are modeled in different ways.

Acknowledgement

Dr. Bengt Hallstedt is acknowledged for many valuable discussions and important contributions.

Database Revision History

If you are interested in the revision history for this or other databases, the information is available in the online help (from Thermo-Calc go to **Help>Online Help**) or in the release notes on our website. For the TCFE (TCS Steel and Fe-alloys) database there is a dedicated page with the history of its development.

TCFE10 Assessed Binary Systems

The 308 binary systems. Green shaded cells are added from the last version of the database to the latest version of the database (53 in total) and yellow shaded cells are updated systems (15 in total).

	Al	B	C	Ca	Ce	Co	Cr	Cu	Fe	Mg	Mn	Mo	N	Nb	Ni	O	P	Ru	S	Si	Ta	Ti	V	W	Y	Zn	Zr
Al	Al																										
B	x	B																									
C	x	x	C																								
Ca	x	10	10	Ca																							
Ce	x	x	x	x	Ce																						
Co	x	x	x	10	x	Co																					
Cr	x	x	x	10	x	x	Cr																				
Cu	x	10	x	x	x	x	x	Cu																			
Fe	x	x	x	x	x	x	x	x	Fe																		
Mg	x	10	10	10	x	10	x	x	x	Mg																	
Mn	x	x	x	x	x	x	x	x	x	x	Mn																
Mo	x	x	x	10	x	10	x	x	x	10	x	Mo															
N	x	x	x			x	x	10	x	10	x	x	N														
Nb	x	x	x	10		x	x	x	x	10	x	x	x	Nb													
Ni	x	x	x	10	x	x	x	x	x	x	x	x	10	x	Ni												
O	x		x		x	10	x	x	x	x	x	10	x	x	x	O											
P	x		x			10	x	x	x		x	x		x	x		P										
Ru	10	10	10	10		10	10	10	10	10	10	10		10	10			Ru									
S	10		10	x	x	10	x	x	x	x	x	10		10	x	10	10	10	S								
Si	x	x	x	x	x	x	x	x	x	x	x	x	10	10	10	x	x	10	10	Si							
Ta	x	x	x			x	x	10	x		x	x	x	x	x			10		x	Ta						
Ti	x	x	x			x	x	x	10	10	x	x	x	x	10	x	x	10	x	x	x	Ti					
V	x	x	x		x	x	x	x	x	10	x	x	x	x	x			10	10	x	10	x	V				
W	x	x	x			x	x	x	10	10	10	x	x	x	x		10		10	x	x	x	x	W			
Y	x	x	x	10	x	x	x	x	x	10	x	x		x	x	x			10	x	x	x	x	x	Y		
Zn	x		x	x	x	x	x	x	x	x	x	x			10		x	10	x	x		x	x		x	Zn	
Zr	x	x	x	10	x	x	x	x	x	x	x	x	x	x	x	x			x	x	x	x	x	x	x	x	Zr

TCFE10 Assessed Ternary Systems

The 269 ternary systems. Systems in the table marked with one asterisk (*) are added since the previous version of the database (13 in total) and systems marked with two (**) are updated systems (15 in total).

Al-Ca-Fe	Al-Mg-O	B-Fe-Si	C-Co-Ni	C-Fe-S	Co-Cu-Fe
Al-Ca-O	Al-Mg-Si	B-Fe-Ti	C-Co-Ti	C-Fe-Si	Co-Fe-Mo**
Al-Ca-Si	Al-Mg-Zn	B-Fe-V	C-Co-W	C-Fe-Ti	Co-Fe-N
Al-C-Fe	Al-Mn-Ni	B-Fe-W	C-Co-Zn	C-Fe-V	Co-Fe-P*
Al-C-Mn	Al-Mn-O	B-Fe-Zr	C-Cr-Fe	C-Fe-W	Co-Fe-S*
Al-Co-Fe	Al-Nb-Ni	B-Mo-Ni	C-Cr-Mn	C-Mn-Si	Co-Fe-Si*
Al-Co-Ni	Al-Nb-Ti	B-Mo-Ti	C-Cr-Mo	C-Mn-V	Co-Fe-W
Al-Co-Zr	Al-Ni-O	B-Ni-Si	C-Cr-N	C-Mo-N	Co-Nb-Si
Al-Cr-Fe	Al-Ni-Ti	B-Ni-Ti	C-Cr-Nb	C-Mo-Nb	Co-Ni-W
Al-Cr-Ni	Al-Ni-Zr	B-Ni-Zr	C-Cr-Ni	C-Mo-Ta	Co-P-W*
Al-Cr-O	Al-O-Si	B-Ti-Zr	C-Cr-Si	C-Mo-Ti	Co-Si-Ti
Al-Cr-Zn	Al-O-Ti	Ca-Cr-O	C-Cr-Ta	C-Mo-V	Co-Si-W
Al-Cu-Fe	Al-O-Y	Ca-Cr-S	C-Cr-V	C-Mo-W	Co-Ti-Zr
Al-Cu-Mn	Al-Ti-V	Ca-Fe-O	C-Cr-W	C-Mo-Zr	Co-W-Zr
Al-Cu-Ni	B-C-Fe	Ca-Fe-S	C-Cr-Zr	C-Nb-Ti	Cr-Cu-Fe
Al-Fe-Mn	B-Co-Fe	Ca-Mg-O	C-Cu-Fe	C-Nb-V	Cr-Cu-Mo
Al-Fe-N	B-Cr-Fe	Ca-Mg-S	Ce-O-S	C-Nb-W	Cr-Cu-Ni
Al-Fe-Ni	B-Cr-Mn	Ca-Mn-O	C-Fe-Mn	C-Ni-W	Cr-Cu-W
Al-Fe-O	B-Cr-Mo	Ca-Mn-S	C-Fe-Mo	C-N-Nb	Cr-Fe-Mn**
Al-Fe-P	B-Cr-Ni	Ca-Ni-O	C-Fe-N	C-N-Ti	Cr-Fe-Mo
Al-Fe-S*	B-Fe-Mn	Ca-O-Si	C-Fe-Nb	C-N-Zr	Cr-Fe-N**
Al-Fe-Si	B-Fe-Mo	C-Co-Cr	C-Fe-Ni	Co-Cr-Fe	Cr-Fe-Nb**
Al-Fe-Ti	B-Fe-Nb	C-Co-Fe	C-Fe-O	Co-Cr-Ni	Cr-Fe-Ni**
Al-Fe-Zn	B-Fe-Ni	C-Co-Nb	C-Fe-P	Co-Cr-W	Cr-Fe-O

Cr-Fe-P
Cr-Fe-Ru*
Cr-Fe-S
Cr-Fe-Si
Cr-Fe-V
Cr-Fe-W
Cr-Fe-Zn
Cr-Mg-O
Cr-Mn-Mo
Cr-Mn-N**
Cr-Mn-Ni
Cr-Mn-O
Cr-Mn-S
Cr-Mn-Si
Cr-Mo-N
Cr-Mo-Ni
Cr-Mo-Si
Cr-Nb-Ni
Cr-Nb-Si
Cr-Ni-O
Cr-Ni-Ru*
Cr-Ni-Si*
Cr-Ni-W
Cr-Ni-Zr
Cr-N-Nb
Cr-N-Ni**
Cr-N-Si
Cr-N-Ti
Cr-N-V
Cr-N-W

Cr-O-Ti
Cr-O-Y
Cr-Si-Ti
Cr-Si-W
C-Si-Ti
C-Ta-W
C-Ti-V
C-Ti-W
C-Ti-Zr
Cu-Fe-Mn
Cu-Fe-Mo
Cu-Fe-N
Cu-Fe-Ni
Cu-Fe-P
Cu-Fe-S
Cu-Fe-Si
Cu-Fe-W*
Cu-Mn-Ni
Cu-Mn-S
Cu-O-Y
C-V-W
C-V-Zr
C-W-Zr
Fe-Mg-O
Fe-Mg-S
Fe-Mn-Mo**
Fe-Mn-N**
Fe-Mn-Nb
Fe-Mn-Ni
Fe-Mn-O

Fe-Mn-P
Fe-Mn-S
Fe-Mn-Si
Fe-Mn-V
Fe-Mo-N
Fe-Mo-Ni**
Fe-Mo-P
Fe-Mo-Si**
Fe-Mo-V
Fe-Mo-W
Fe-Nb-O
Fe-Nb-P
Fe-Nb-Si**
Fe-Nb-V
Fe-Nb-Zr
Fe-Ni-O
Fe-Ni-P
Fe-Ni-Si**
Fe-Ni-Ti*
Fe-Ni-W
Fe-N-Nb
Fe-N-Ni**
Fe-N-Ti
Fe-N-V
Fe-N-W**
Fe-O-S
Fe-O-Si
Fe-O-Y
Fe-P-Si
Fe-P-Ti

Fe-P-W*
Fe-Si-Ti
Fe-Si-W
Fe-Si-Zr
Fe-S-Ti
Fe-S-W*
Fe-Ti-Zr
Mg-Mn-O
Mg-Mn-S
Mg-Ni-O
Mg-O-Si
Mn-Mo-Ni
Mn-Mo-Si
Mn-Ni-O
Mn-Ni-Si
Mn-O-S
Mn-O-Si
Mn-O-Y
Mn-Si-Zn
Mo-Ni-Si
Mo-N-Ni
Mo-N-V
Ni-O-Si
Ni-O-Ti
Ni-O-Y
Ni-P-W*
Ni-Si-Ti
Ni-Si-W
Ni-Si-Zr
N-Nb-Ti

N-Nb-V
N-Ti-V
N-V-W
O-Si-Y
O-Y-Zr

TCFE10 Assessed Quaternary Systems

The 77 quaternary systems. Systems in the table marked with one asterisk (*) are added since the previous version of the database (1 in total) and systems marked with two (**) are updated systems (2 in total).

Al-C-Fe-Mn
Al-Ca-Mg-O
Al-Ca-O-Si
Al-Cr-Fe-Ni
Al-Cr-Fe-O
Al-Cr-Fe-Zn
Al-Cr-Mg-O
Al-Cr-Mn-O
Al-Cr-Ni-O
Al-Cr-O-Y
Al-Fe-Mg-O
Al-Fe-Mn-O
Al-Fe-Ni-O
Al-Fe-O-Y
Al-Mg-Mn-O
Al-Mg-Ni-O
Al-Mg-O-Si
Al-Mn-Ni-O
Al-Mn-O-S
Al-O-Si-Y
B-Cr-Fe-Mo
C-Co-Cr-W
C-Co-Fe-Mo**
C-Co-Fe-Ni

C-Co-Fe-W
C-Co-Nb-W
C-Co-Ni-W
C-Co-V-W
C-Cr-Fe-Mn
C-Cr-Fe-Mo
C-Cr-Fe-N
C-Cr-Fe-Ni
C-Cr-Fe-V
C-Cr-Fe-W
C-Cr-Mn-V
C-Cr-Mn-W
C-Cr-Mo-V
C-Cr-V-W
C-Fe-Mn-Nb
C-Fe-Mn-Si
C-Fe-Mo-Nb
C-Fe-Mo-Si
C-Fe-Mo-V
C-Fe-Mo-W
C-Fe-N-Ni
C-Fe-Nb-W
C-Fe-Ni-W
C-Fe-Si-W

C-Fe-V-W
C-Mo-N-Ni
C-N-Nb-Ti
C-N-Nb-V
C-N-Ti-V
Ca-Fe-Mg-S
Ca-Fe-Mn-S
Ca-Fe-O-Si
Ca-Mg-O-Si
Cr-Fe-Mg-O
Cr-Fe-Mn-N**
Cr-Fe-Mn-O
Cr-Fe-Mo-N
Cr-Fe-N-Nb
Cr-Fe-N-V
Cr-Fe-Ni-O
Cr-Fe-O-Y
Cr-Mg-Mn-O
Cr-Mg-Ni-O
Cr-Mn-Ni-O
Cr-Mo-N-Nb
Cr-N-Ni-Si*
Fe-Mg-Mn-O
Fe-Mg-Ni-O

Fe-Mg-O-Si
Fe-Mn-Nb-N
Fe-Mn-Ni-O
Mg-Mn-Ni-O
Mn-O-Y-Zr

TCFE10 Calculation Examples

Validation of the TCFE10 database against experimental data shows accurate predictions for various applications. Below are a few notes about some specific applications.

The examples shown below have been calculated with various versions of the TCFE database, so small differences might be observed if they are recalculated with TCFE10. However, for the systems which have been considerably changed , the results should have already been updated.

Nitrogen Alloyed Duplex Stainless Steels (DSS)

The duplex steels are designed to solidify in the single-phase ferritic mode with formation of austenite by precipitation in the solid state [1992 Nilsson, 2017 Petterson]. The high-temperature phase equilibria calculations with TCFE (TCFE10) show the interval below solidus where the material is fully ferritic (Figure 1).

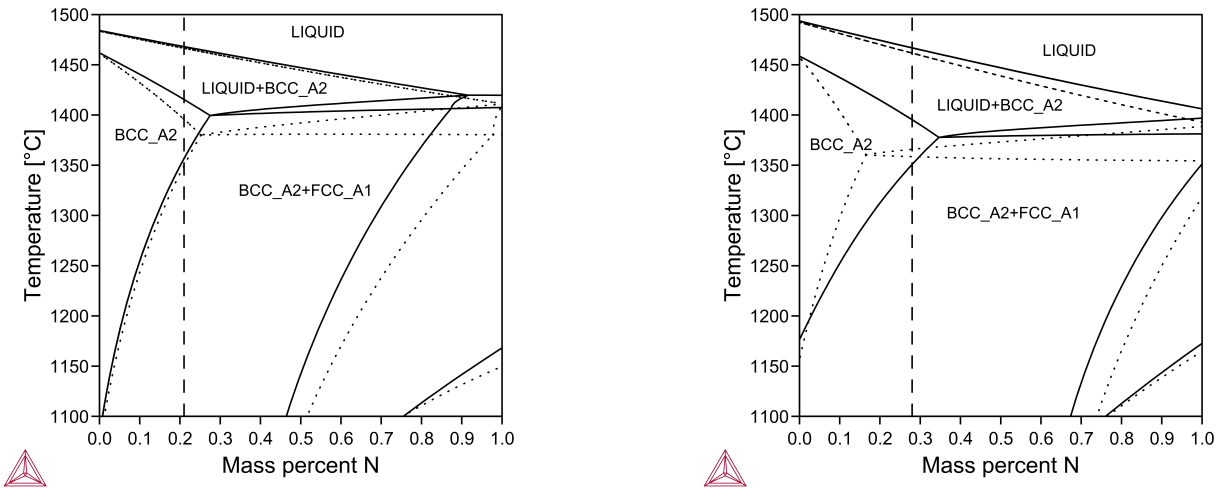

Figure 1: Calculated isopleth sections for 2101 grade (left) and 2507 grade (right) with nitrogen contents up to 1 wt. % using the TCFE10 database (solid lines) compared with TCFE9 (dotted line). The nitrogen content of the alloy is indicated by the dashed lines.

The TCFE database can also be used to calculate the limits of nitrogen solubility in austenite and ferrite at various nitrogen activities as shown in Figure 2.

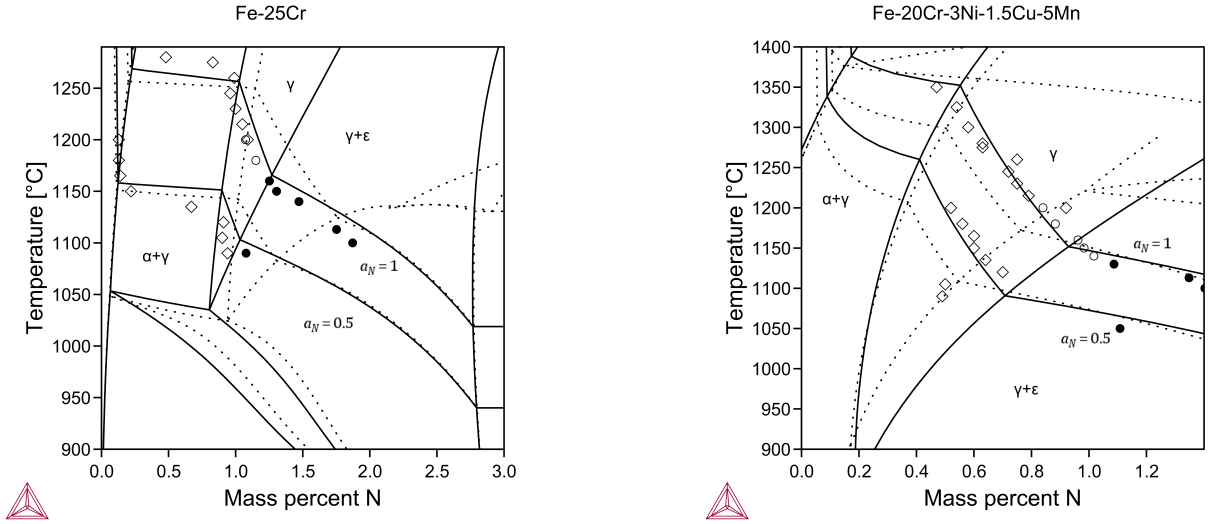

Figure 2: Isopleth for the Fe-25Cr (left) and Fe-20Cr-5Mn-3Ni-1.5Cu-N (right) system calculated with TCFE10 (solid lines) showing the phase regions of main interest and the isoactivity line a_N = 1 and the iso-activity line for a_N=0.5. Using the TCFE10 database (solid lines) compared with TCFE9 (dotted line). Experiments from FROST project – Internal report.

The η-silicide (η-nitride) has a diamond cubic structure with typical composition Cr_3Ni_2SiN. Experimental information found in the literature together with new experimental information within internal projects were used to assess the thermodynamic description of the η- silicide (ETA_M5SIN). In Table 1 the composition of some studied alloys are shown and in Table 2 a comparison is made between observed and calculated composition of η-silicide.

Table 1. Composition (wt. %) of two of the alloys studied by Pettersson (1998).

Alloy	C	Si	Mn	P	S	Cr	Ni	Mo	N
B3	0.014	0.54	1.44	0.009	0.003	19.8	25.0	4.59	0.21
L3	0.014	0.56	5.24	0.012	0.004	20.2	18.5	4.28	0.44

Table 2. Comparison between measured and calculated composition of η-silicide in alloys B3 and L3 at 800 °C [1998 Pettersson].

Alloy	at. %	Cr	Ni	Mo	Fe	Si	N
B3	Exp.	30	25.5	12	5	13	14.5
	Calc.	27.7	25.8	15.2	2.8	14.3	14.3
L3	Exp	24 25.1	25.0 24.7	15.0 15.2	4.5 8.0	13 (14.3)	18.5 (14.3)
	Calc.	28.6	26.3	14.3	2.3	14.3	14.3

Viscosity of the Metallic Liquid

In the TCFE10 database, the viscosity of metallic liquid alloys is modeled as follows:

$$RT\ln\eta = RT\ln\eta_0 + E$$

where η is the dynamic (or shear) viscosity of the liquid and η_0 is the viscosity at finite temperatures, *E* is the activation energy in J/mole, *R* is the gas constant and *T* absolute temperature. The SI unit of viscosity is pascal.second (Pa.s). The viscosity parameters are expanded via Redlich-Kister polynomials. Example: Viscosity of a liquid A-B alloy is:

$$RT\ln\eta_{alloy} = x_A(E_A + RT\ln\eta_0^A) + x_B(E_B + RT\ln\eta_0^B) + x_A x_B[L_0 + (x_A - x_B).L_1]$$

The two first terms are the contributions for the end-members, *A* and *B* elements and the last term accounts for the excess viscosity. Basically, we optimize the activation energies. L_0, L_1 and etc. are the parameters that are optimized to fit the viscosity data.

The kinematic viscosity, ν, is the ratio of the dynamic viscosity to the density, ρ, of the alloy:

$$\nu = \frac{\eta}{\rho}$$

The SI unit of kinematic viscosity is square meter per second (m^2s).

The viscosity curves of Fe-Ni and Cr-Ni systems at 1873 K and a comparison to experimental data are shown in Figure 3.

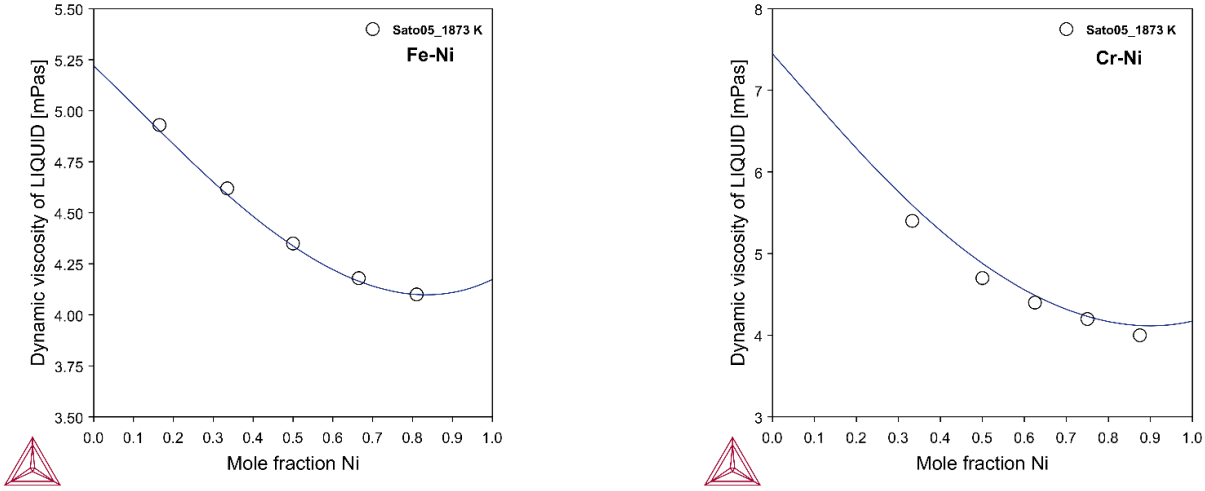

Figure 3: Isoviscosity curve for Fe-Ni system at 1873 K (left). Experimental data is from [2005 Sato] compared to isoviscosity curve of Cr-Ni system at 1873 K (right). Experimental data is from [2011 Sato].

The viscosity of Cr-Fe-Ni ternary system at 1800 K is calculated from assessed binary parameters and is shown in Figure 4.

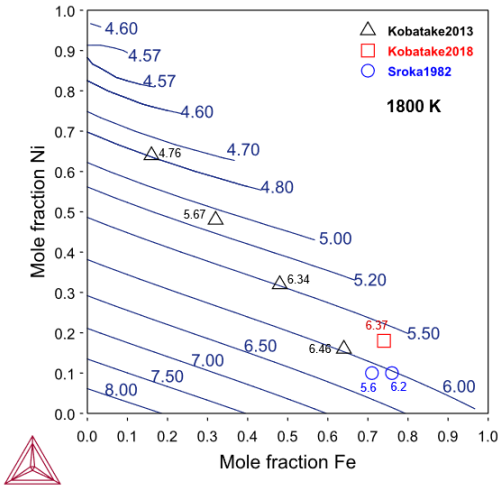

Figure 4: Isoviscosity of Cr-Fe-Ni at 1800 K. Experimental data is from [2013 Kobatake, 2018 Kobatake, 1982 Sroka].

In Console Mode, the viscosity can be plotted via a step calculation vs. temperature or composition. The relevant property is VISC of the liquid phase. The calculated VICS property is not the viscosity (η) but is related to η via $R*T*\ln*\eta$, thus in order to plot the viscosity or η, one needs to define a function for η as follows:

$$\eta = exp(VISC(LIQUID)/(R*T)) \text{ [Pa.s]}$$

In Graphical Mode, the viscosity (η) is directly plotted via the one axis calculation type.

Ordered Phases

The ordered phases BCC_B2 and FCC_L12 are described with a two sub-lattice model using a single Gibbs energy curve which enables order/disorder transformations to be modeled as described by [2001, Dupin].

In TCFE10 the disordered part of BCC_B2 and FCC_L12 (A2_BCC and A1_FCC respectively) are identical to the ordinary BCC_A2 and FCC_A1, but only 1 J/mole of formula unit less stable. This way the ordered phases BCC_B2 and FCC_L12 are split from the disordered BCC_A2 and FCC_A1, and the second order phase transitions are automatically displayed by a narrow first order transition (Figure 5).

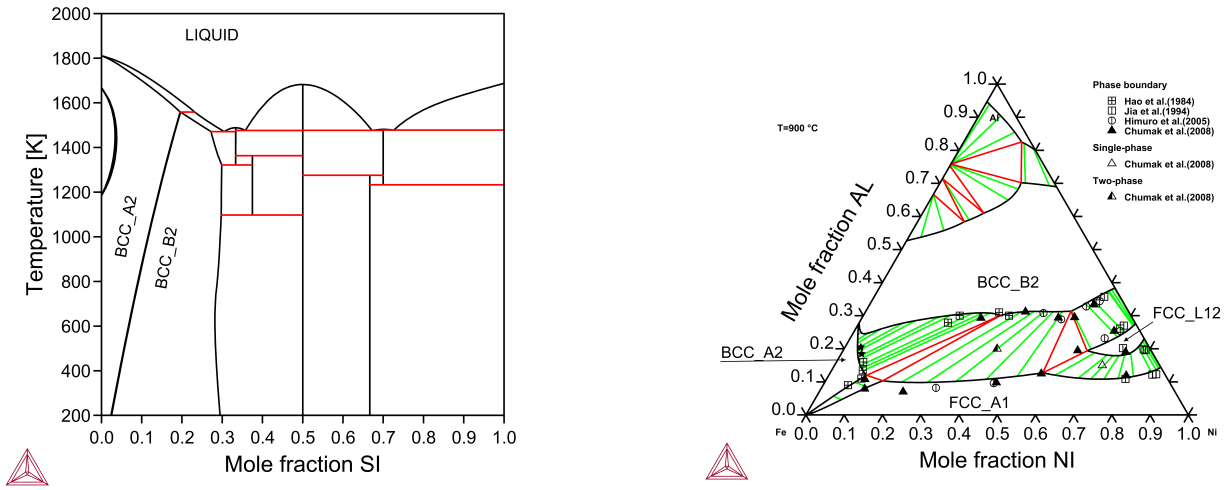

Figure 5: Fe-Si phase diagram (left) and isothermal section of Al-Fe-Ni phase diagram at 1173 K (right).

Sulphurous Systems

The formation of sulfides in steels can be detrimental or beneficial. In either case it is important to

understand and control the formation of sulfides. In the TCFE9 database the thermodynamics of Ca-Fe-Mn-Mg-S and its lower order systems are updated after the work by Dilner [2016] (Figure 6). The Cr solubility in MnS is estimated based on the experimental data. Cu-sulfides are also added for some applications such as electrical steels.

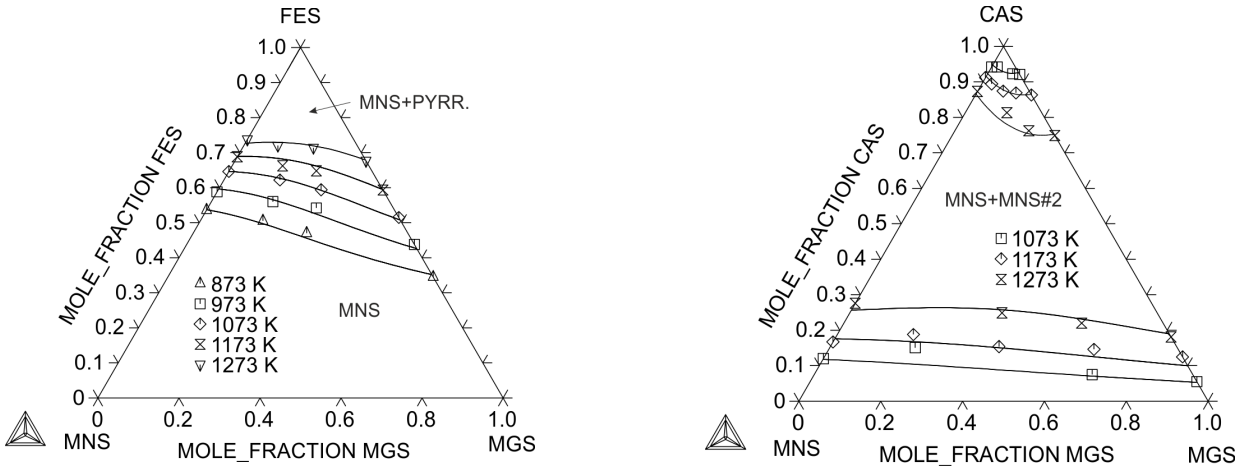

Figure 6: The solubility lines in the FeS-MnS-MgS system in the temperature interval 873-1273 K (left). The CaS-MgS-MnS isothermal sections plotted at 1073-1273 K together with experimental information as cited in [2016, Dilner] (right).

Phosphorus Systems

A series of new experimental data and thermodynamic assessments regarding the phosphorus containing systems have become available by [2014a, 2014b and 2015, Miettinen]. Thereafter, several phosphorus containing ternary iron-based systems, Fe-X-P (X=Al, Cr, Mn, Mo, Nb, Ni, Ti, Si) are included in the TCFE9 database.

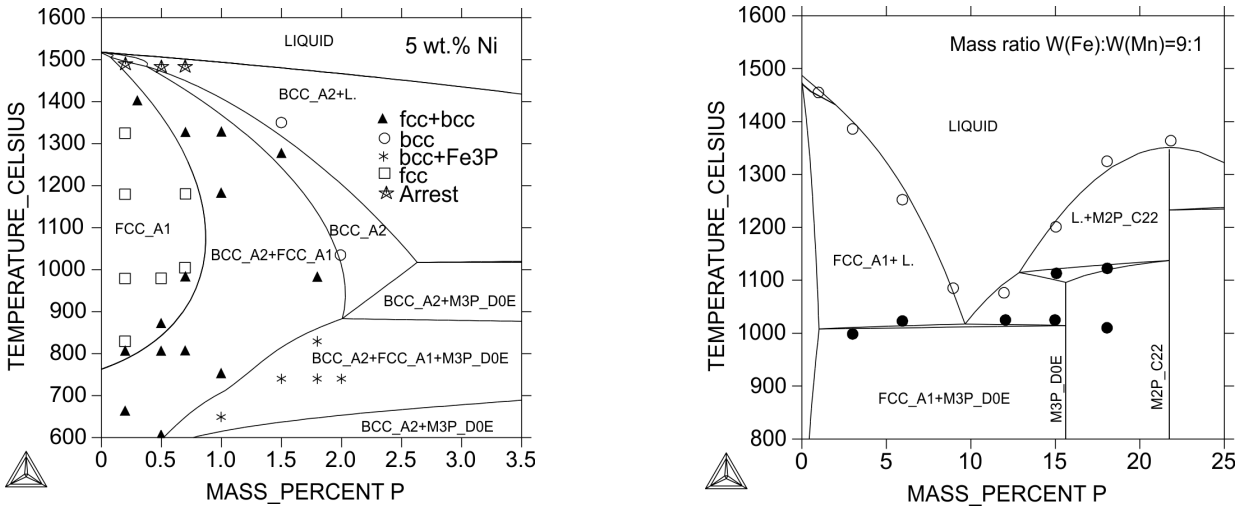

Figure 7: The vertical section of the Fe-Ni-P system at 5 wt.% Ni, together with experimental data as cited in [2015, Miettinen] (left). Calculated vertical section of the Fe-Mn-P system at mass ratio W(Fe):W(Mn)=9:1, together with experimental data as cited in [2014b, Miettinen] (right).

Boron-containing Systems

Thermodynamic description of many boron containing systems are revised including iron containing ternary systems, Fe-X-B (X=C, Cr, Co, Mo, Mn, Nb, Ni, Si, Ti, V, W, Zr), and also some other ternary systems such as B-Cr-Mo, B-Cr-Ni, B-Ni-Si and the quaternary B-Cr-Fe-Mo system.

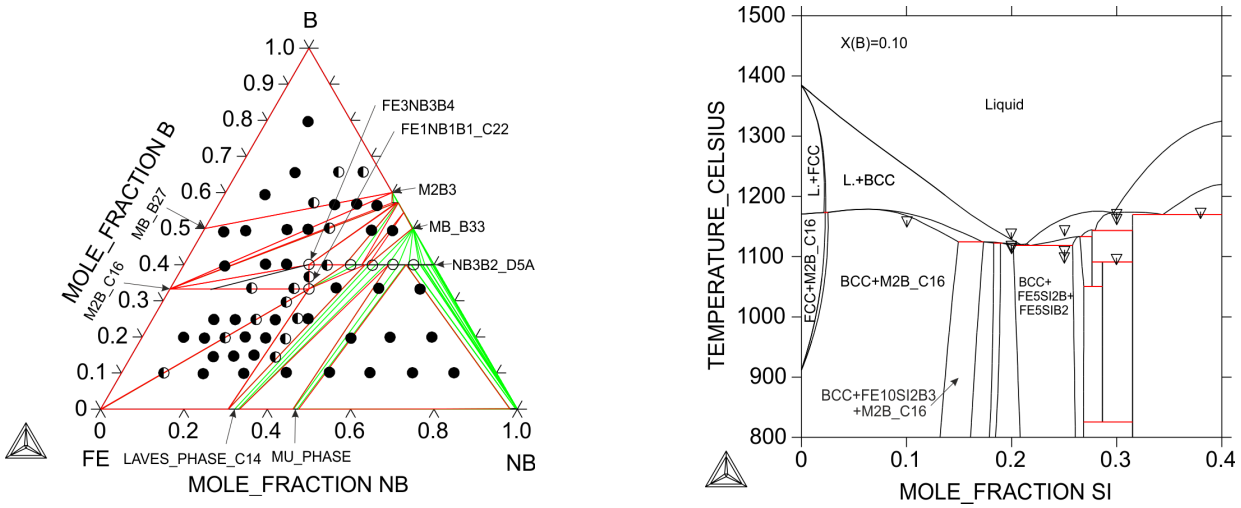

Figure 8: A calculated isothermal section diagram of the Fe–Nb–B system at 1073 K, compared with the experimental phase fields [2008, Yoshitomi] (left). Calculated Fe-Si-B isopleth at X(B)=0.10 with DSC data [2013, Poletti] (right).

Laves Phase

In the TCFE9 database, vanadium (V) is added in the Laves phase and the solubility of many elements are revised. The Laves phase is modified in Fe-Nb, Cu-Mo, Cu-Nb, Cu-W, Mo-Si, Nb-Si, Cu-Fe-Mo, Cr-Fe-Mo, Cr-Si-Nb, Fe-Mn-Mo, and Fe-Mo-Si systems. This description shows satisfying accuracy of the predictions compared to experimental information [2008, Zhang; 2000, Wang].

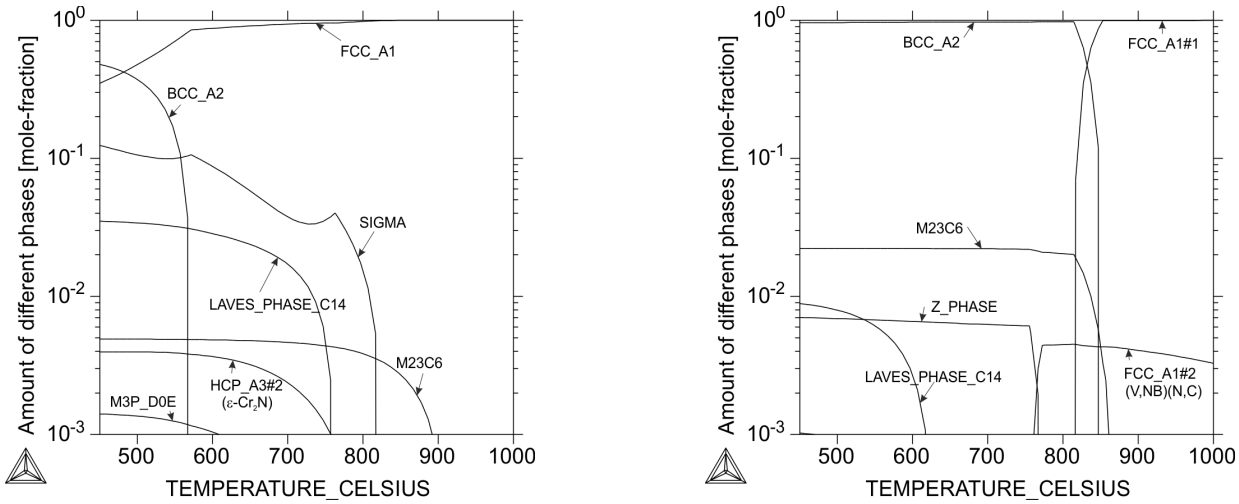

Figure 9: Amount of different phases as a function of temperature in two commercial steels 316L [2004, Sahlaoui] (left) and P91 [2010, Panait] (right).

Copper-containing Systems

The thermodynamic properties of Cu contacting systems is improved in TCFE9 and later versions by adding several new descriptions including Ca-Cu, Cu-Nb, Cu-W, Al-Cu-Fe, Al-Cu-Mn, Al-Cu-Ni, Cr-Cu-Mo, Cr-Cu-W, Cu-Fe-Mn (Figure 10a), Cu-Fe-Mo (Figure 10b) and Cu-Mn-Ni systems.

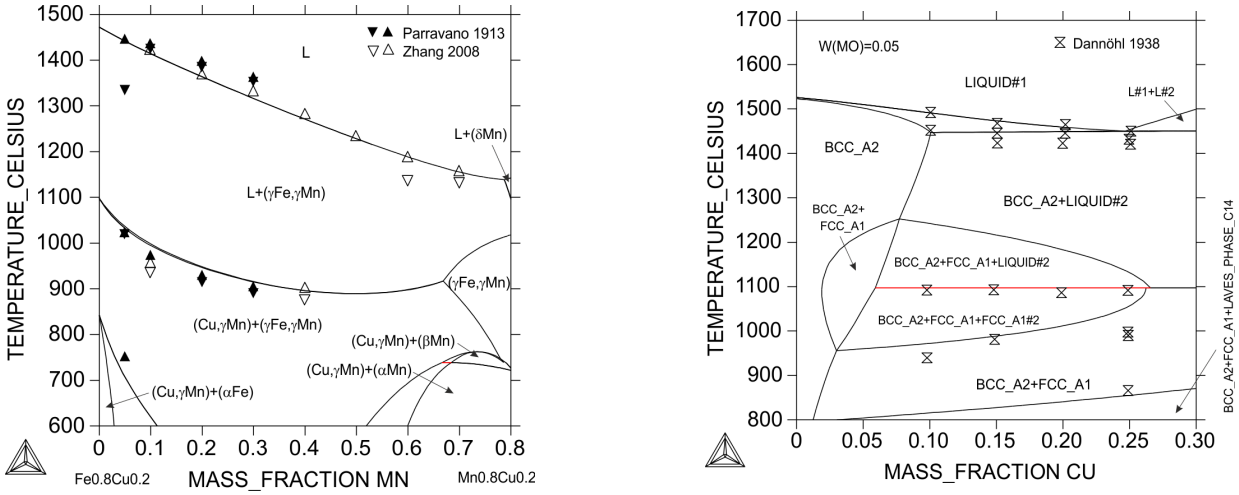

Figure 10: Calculated vertical sections of the Cu-Fe-Mn system at 20 wt.% Cu [2008, Zhang] (left) and Cu-Fe-Mo system at 5 wt.% Mo along with the experimental data [2000, Wang] (right).

Nb and V-containing Systems

Niobium (Nb) and vanadium (V) are common alloying elements in different types of steels with high affinity to form carbides and nitrides. In the TCFE9 several Nb and V systems are either newly added (such as Mn-Nb and Fe-Mn-Nb (Figure 11 left) systems) or updated (including C-Nb, Fe-Nb, Fe-V, Nb-V, C-Cr-Nb, and Fe-Nb-V (Figure 11 right)).

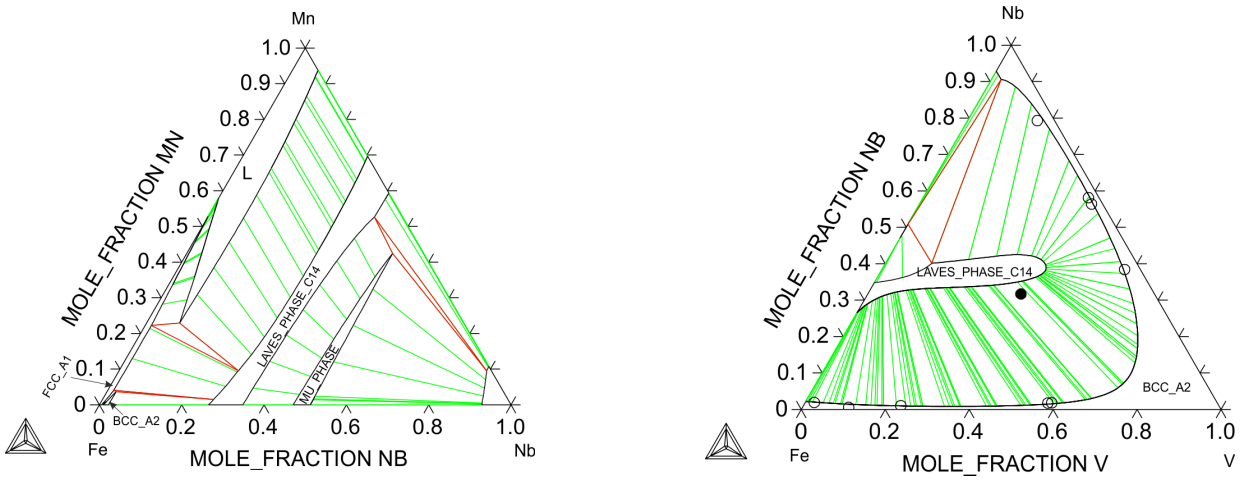

Figure 11: Isothermal sections of Fe-Mn-Nb [2013a, Khvan] (left) and Fe-Nb-V [2013b, Khvan] systems at 1573 K (right).

Advanced High-strength (AHS) Steels Containing Al, Mn, Si, and C

High temperature equilibria, and specifically the peritectic reaction, is of significant importance in continuous casting practice. The TCFE9 database is improved by using data from latest thermodynamic assessments [2017, Zheng] and systematic DSC measurements in C-Fe-Mn-Si and Al-C-Fe-Mn-Si systems [2016, Presoly and 2015, Moon].

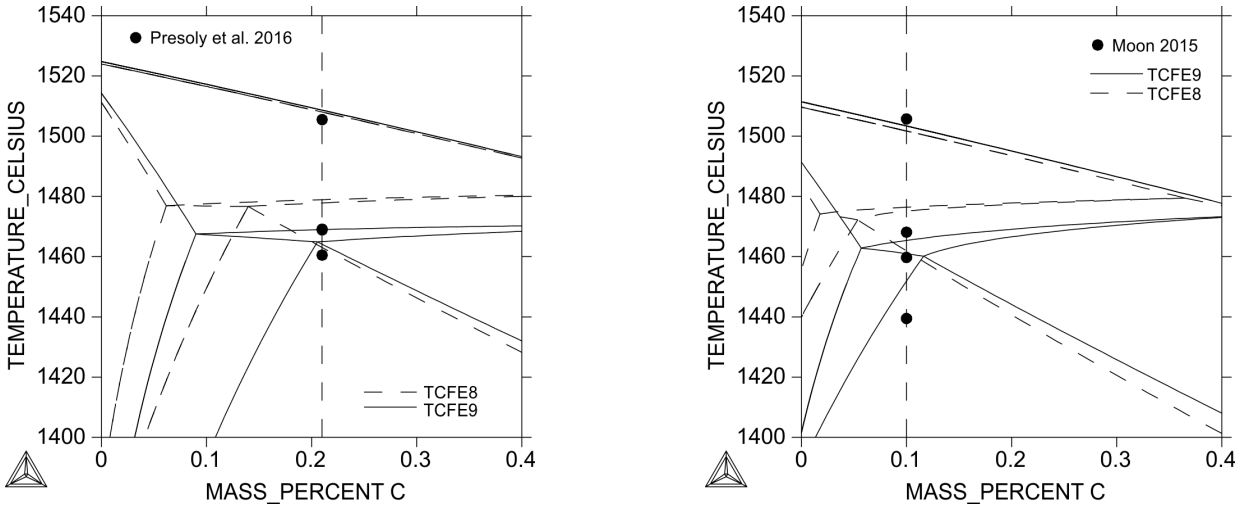

Figure 12: Calculated isoplethal section of Fe-2.12Mn-0.77Al-0.54Si-xC (left) and Fe-2.75Mn-1.11Si-0.097Al-0.014Ti-0.02Nb-xC (right).

Low-density Steels

Reducing the weight of engineering structures saves both material and energy, and also leads to greater fuel efficiency and reduces emissions in automobiles.

The Al-C-Cr-Fe-Mn-Ni systems is the core of low density steels and allows studies to replace costly Ni and Cr in stainless steels by cheaper Mn and Al. In the TCFE9 database the Al-C-Cr-Fe-Mn-Ni and its subsystems are updated with the latest assessments and experimental info. The Kappa phase is described with a regular CEF model and extended with Mn. Manganese phases CBCC_A12 and CUB_A13 are also added.

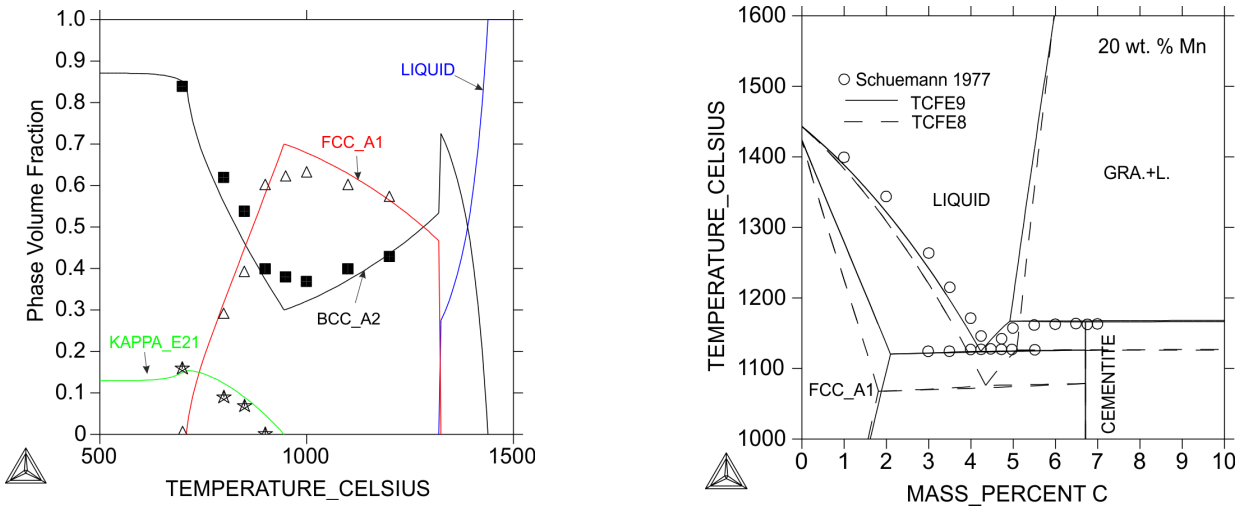

Figure 13: The mole fraction change of each phase with the temperature for Fe-10Mn-10Al-0.7C low-density steel [2016, Zhao] (left). The calculated vertical section of C-Fe-Mn involving the liquid phase at 20 wt.% Mn [2011, Djurovic] (right).

Kim et al. [2015] showed that a B2-type brittle but hard intermetallic compound can be effectively used as a strengthening second phase in high-aluminum low-density steel. The table shows the result of a calculation with the TCFE9 database compared with the experimental observations of Kim et al. [2015].

Table 3. Partitioning of alloying elements between B2 precipitate and austenite matrix in during annealing of cold rolled Fe-10Al-15Mn-0.8C-5Ni (at.%). Calculation with the TCFE9 database vs. experimental data [2015, Kim].

	FCC_A1 composition (at.%)		**B2_BCC composition (at.%)**	
Element	**Calculated**	**Experiment [Kim, Kim and Kim, 2015]**	**Calculated**	**Experiment [Kim, Kim and Kim, 2015]**
Fe	65.6	68	53.7	57
Al	15.1	13	25.5	22.6
Mn	16.8	16.6	10.2	9.4
Ni	1.9	2.4	10.1	11.0

Martensite Formation

The TCFE database has been successfully used for thermodynamically-based prediction of the lath and plate martensite start temperature [2012, Stormvinter]. The Ms temperature prediction depends on the available driving force which should be equal to the barrier for Martensite formation. In the TCFE9 database particular attention is paid to the epsilon (ε) martensite transformation, and the thermodynamic descriptions of Fe-Mn-C system is modified to give a reasonable driving force for the γ→ε diffusionless transformation. As a result, the database can be used with the Martensite start temperature model available in Property Models for steels, to predict the Ms temperature (Figure 14).

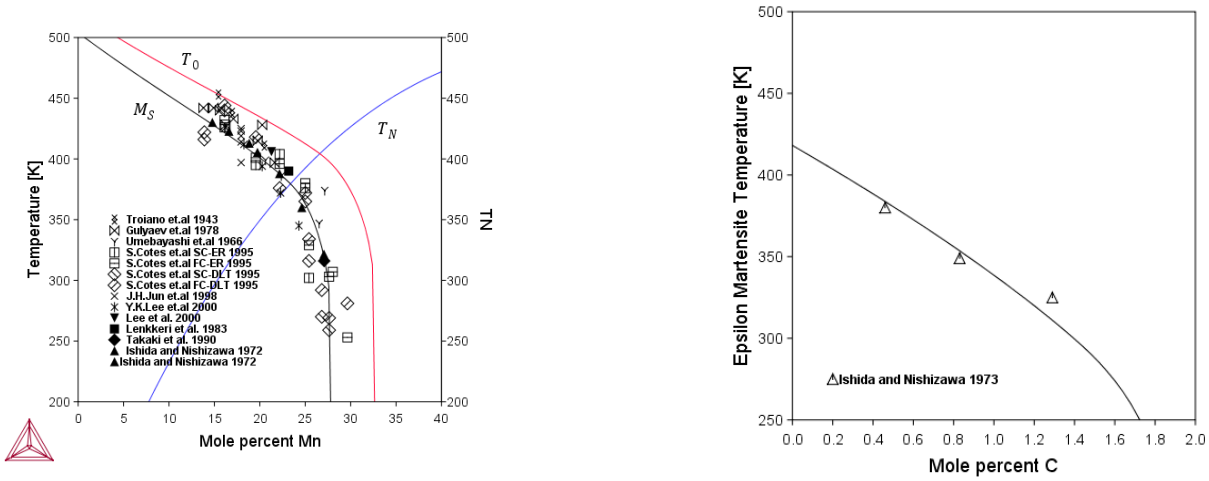

Figure 14: Epsilon martensite start temperature for Fe-Mn (left) and Fe-17at.% Mn-xC (right).

Oxidation

The description of the SPINEL, HALITE and CORUNDUM phases and more, for the Fe-Al-Ca-Cr-Mg-Mn-Ni-Si-Ti-C-O system [2009, Kjellqvist] in the TCFE database (TCFE6 and later versions) allows for accurate predictions in different fields, e.g. oxide scale formation on various steels (Figure 15). In the left-hand side image for this figure, the oxide scale formed on a steel is predicted and the agreement with experimental information [1986, Douglass; 1991, Nanni; 2004, Kurokawa; 1984, Wang] is very good. You can see that below the outer scale (rich in corundum) an Fe-Mn spinel is formed and closest to the substrate a layer with halite and a Cr-Mn rich spinel, which also is verified in the work by Douglass et al. [1986].

The model used for the spinel and corundum phases makes it possible to simulate diffusion inside these phases using the Diffusion Module (DICTRA) (also possible for other oxides such as halite) provided that a suitable mobility database is available.

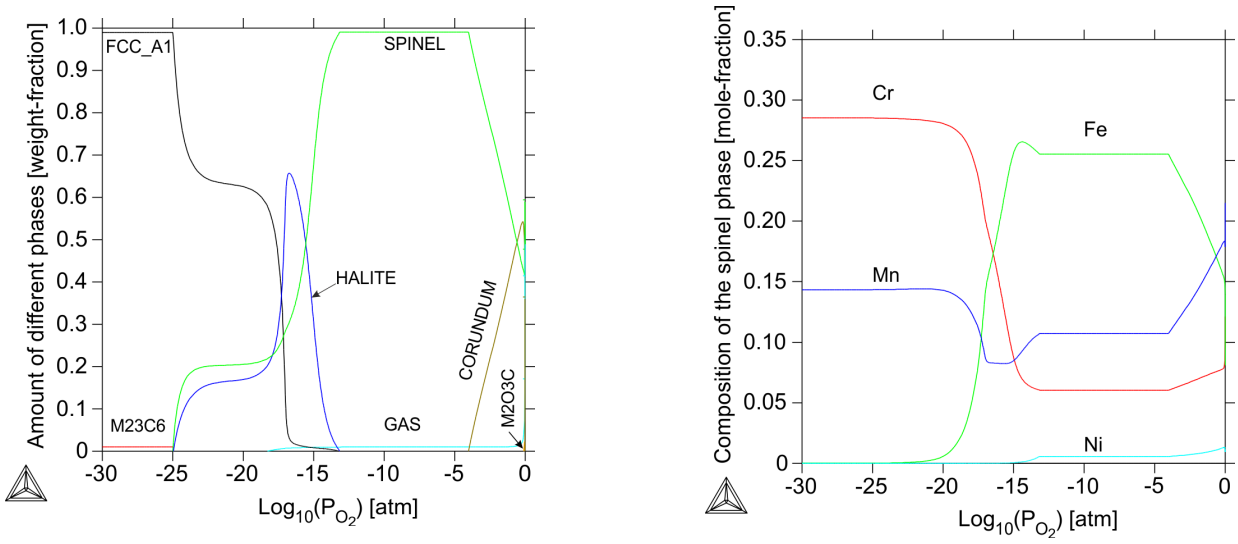

Figure 15: Oxidation of a steel (Fe-17.8Mn-9.5Cr-1.0Ni-0.27C wt.%) at 900 °C (left). Calculated composition of the spinel phase in the oxide scale at 900 °C (right).

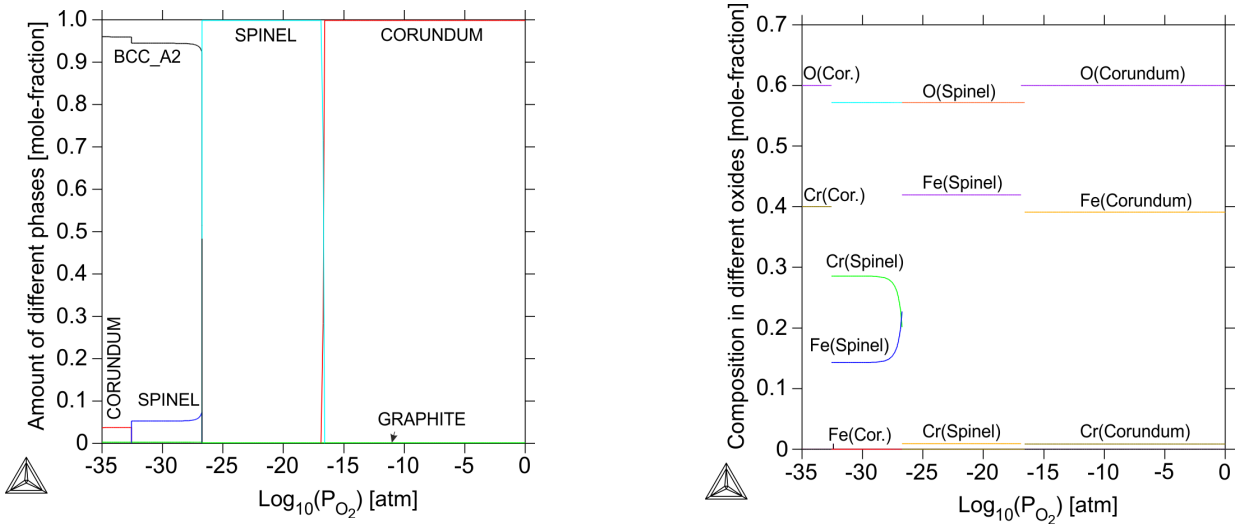

Figure 16: Calculated oxide scale formed on a low-Cr boiler steel (Fe-1.44Cr-0.06C wt.%) at 550 °C (left). Calculated composition in different oxides versus oxygen partial pressure for the same steel as in the first plot (right). These results agree very well compared with experimental information [2005, Trindade]. A small amount of graphite is present for the whole oxygen partial pressure interval.

Oxide Dispersion Strengthened (ODS) Steels

TCFE database (TCFE8 and later versions) includes the element Y, mainly for the purpose of the

development of oxide dispersion strengthened (ODS) steels (Figure 17).

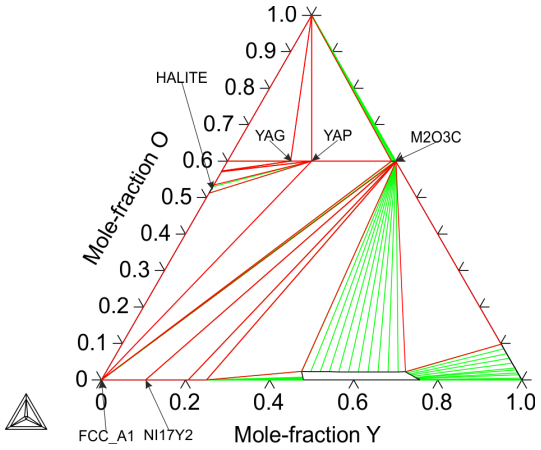

Figure 17: Isothermal section of Fe-Y-O calculated at 1000 °C.

Molar Volumes

The TCFE database (TCFE4 and later versions) contains molar volume data for all phases in the database , allowing for the calculation of volume fraction of phases, as well as density and coefficient of thermal expansion using Thermo-Calc. Molar volumes are also needed when using the Precipitation Module (TC-PRISMA) for precipitation simulations. Validation of predicted densities in different alloys is shown in the left plot in Figure 18. The relative length change of a commercial steel is shown in the right-hand side plot.

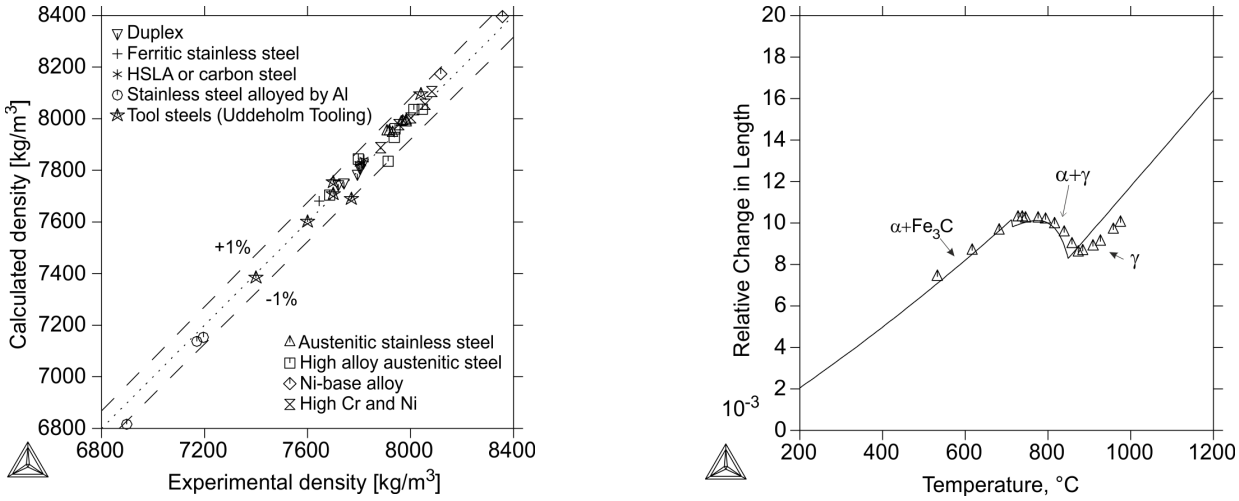

Figure 18: Calculated density of several steels at room temperature compared to experimental data provided by Sandvik [2017] and Uddeholm Tooling [2017] (left). Relative length change [2002, García de Andrés] of steel Fe-0.11C-0.5Mn-0.03Si-0.01Cr-0.02Ni (wt.%) compared with predictions using the TCFE database (right).

Galvanization

TCFE database (TCFE8 and later versions) includes the element Zn, owing to its importance for hot-dip galvanization processes with the focus on the Zn corner of Al-Cr-Fe-Zn system.

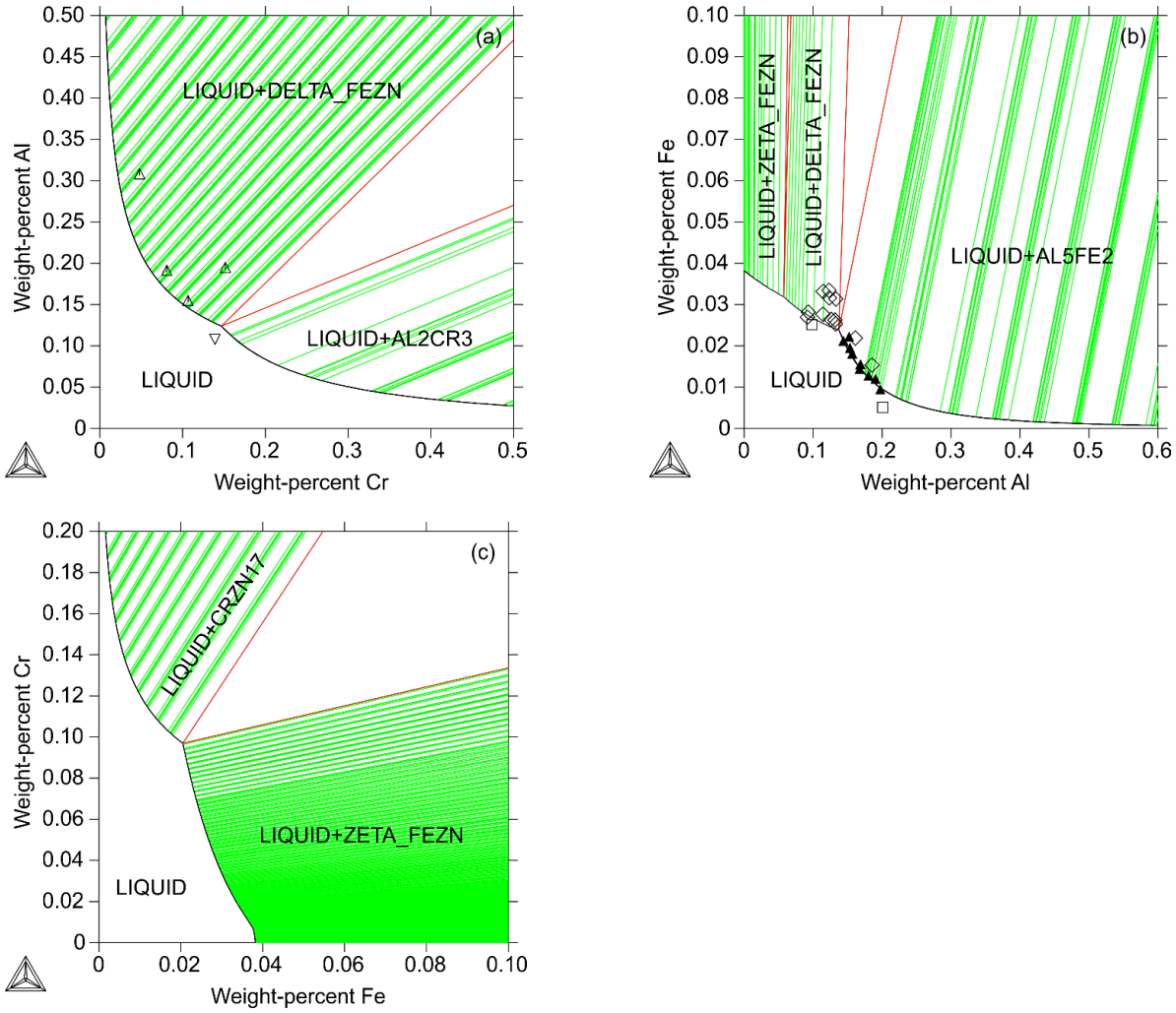

Figure 19: Zn corner of Al-Cr-Zn system (top left), Al-Fe-Zn system (top right), and Cr-Fe-Zn system (bottom left) at 460 °C compared with experimental information [2007, Fourmentin; 2007, Nakano].

Tool Steels and High-speed Steels (HSS)

TCFE database can be used for tool steels and high-speed steels (HSS), especially to predict correct phases and phase compositions. Figure 20 demonstrates the MC, M7C3, and M6C carbides compositions for a number of different tool steels and high-speed steels.

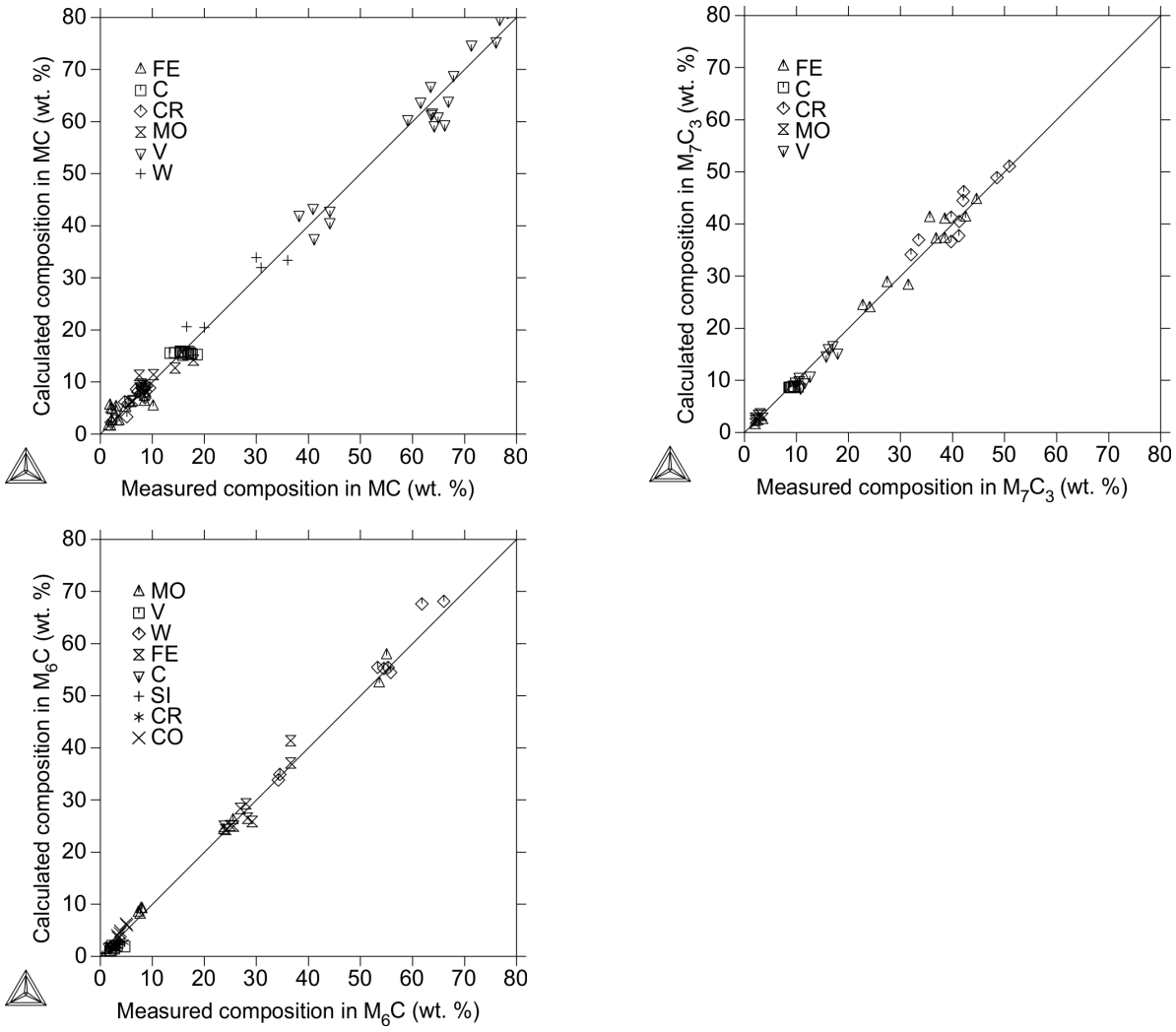

Figure 20: Calculated vs. experimental equilibrium composition for MC carbide (top left), M7C3 carbide (top right) and M6C carbide (bottom left) in different tool steels and high-speed steels. The experimental data is taken from references [2004a, 2004b and 2005 Bratberg].

High-strength Low-alloy Steels (HSLA)

Another application of the database is for high-strength low alloy (HSLA) steels, especially to predict correct phases and phase compositions in all possible precipitates (see Figure 21 and Table 1).

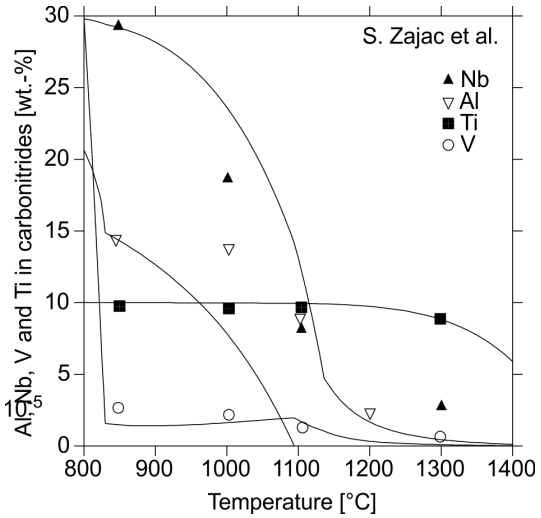

Figure 21: Predicted mass fraction of Nb, Ti, V and Al in precipitates compared with experimental information [1998, Zajac] for a microalloyed steel with 0.09C-1.51Mn-0.035Al-0.010Ti-0.030Nb-0.08V-0.0105N (wt.%).

Table 4. Predicted compositions for $(Ti_xNb_{1-x})N_yC_{1-y}$ and $(Nb_tTi_{1-t})C_uN_{1-u}$ carbonitrides (site fractions) in two microalloyed steels compared with measurements from Craven et al. [2000]. All calculations were made at 1000 °C. Both steels contain the following alloy contents: 0.036Al- 1.4Mn-0.50Ni-0.015P-0.002S-0.4Si (wt.%) in addition to the composition provided in the table.

Steel 1	**0.07C wt.%**	**0.0079N wt.%**	**0.025Nb wt.%**	**0.009Ti wt.%**
	x	y	t	u
Experiment	0.86 ± 0.04	≈ 1	1	≈ 0.7
Calculation	0.94	0.94	0.98	0.71
Steel 2	**0.097%C**	**0.0049%N**	**0.017%Nb**	**0.010%Ti**
	x	y	t	u
Experiment	0.91 ± 0.03	0.84 ± 0.05	1 or ≈ 0.8	≈ 1
Calculation	0.97	0.92	0.97	0.78

Liquidus and Solidus

TCFE datbase can satisfactorily predict the liquidus and solidus temperatures in various commercial steels and model alloys. In addition, the accuracy to predict the correct primary phase to form from the liquid is very high. In Figure 22 some measured liquidus temperatures are compared with the calculated ones for various steels.

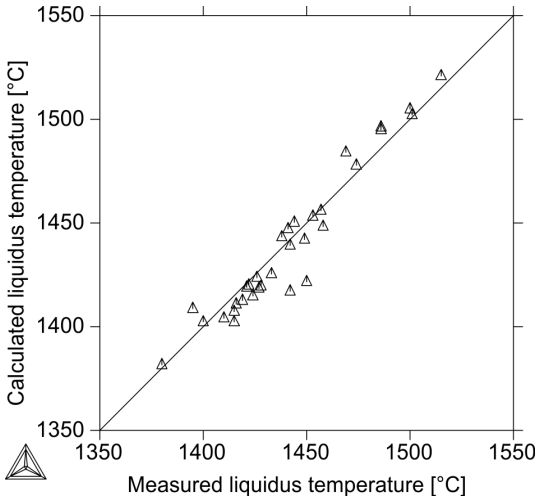

Figure 22: Experimental liquidus temperatures [1977, Jernkontoret; 1997, Allan; 2003, Coelho] for various steels (stainless steels, carbon and low alloy steels, high-speed steels with high Nb content and chromium steels) compared with calculations with the TCFE database.

Cemented Carbides

Although the TCFE database is mainly designed for steels and iron alloys, it can also be used for cemented carbides, especially in predicting correct phases and fractions, phase compositions and invariant solid/liquid equilibrium temperatures, see the table below.

Table 5. Predicted temperatures of invariant solid/liquid equilibria including WC, MC (cubic carbide), and graphite or M6C compared with experimental data [2001, Kruse; 2006, Bratberg].

System	Invariant temperature graphite, °C		Invariant temperature M6C, °C	
	Experimental	Calculated	Experimental	Calculated
Co-W-C	1298	1298	1368	1368
+Nb	1282	1287	1345	1349
+Ta	1289	1289	1352	1348
+Ti	1289	1292	1361	1364
+Zr	1283	1291	1358	1362

TCFE10 References

[1977, Jernkontoret] Jernkontoret, *Guide to Solidification of Steels*, Ljungberg Tryckeri AB, Stockholm, Sweden, (1977).

[1982, Sroka] M. Sroka and J. Skala, "Chemical Composition and Viscosity of Steels." *Freib. Forschungsh. B, Metall. Werkstofftech*, 17-26 (1982).

[1984, Wang] R. Wang, M. J. Straszheim, R. A. Rapp, A high-temperature oxidation-resistant Fe-Mn-Al-Si alloy. *Oxid. Met.* **21**, 71–79 (1984).

[1986, Douglass] D. L. Douglass, F. Gesmundo, C. de Asmundis, The air oxidation of an austenitic Fe-Mn-Cr stainless steel for fusion-reactor applications. *Oxid. Met.* **25**, 235–268 (1986).

[1991, Nanni] P. Nanni, V. Buscaglia, G. Battilana, E. Ruedl, Air oxidation of a Mn-Cr austenitic steel of potential use for fusion reactor structural applications between 1073 and 1473 K at 105 Pa. *J. Nucl. Mater.* **182**, 118–127 (1991).

[1992, Nilsson] J.-O. Nilsson, “Super duplex stainless steels,” *Mater. Sci. Technol.*, **8** (8), 685–700 (1992).

[1997, Allan] G. Allan, “Castability, solidification mode and residual ferrite distribution in highly alloyed stainless steels”, European Commission (1997).

[1998, Pettersson] R.F.A. Jargelius-Pettersson, Precipitation trends in highly alloyed austenitic stainless steels, *Zeitschrift Für Met.*, **89**, 177–183 (1998).

[1998, Zajac] S. Zajac, R. Lagneborg, “Thermodynamic model for the precipitation of carbonitrides in microalloyed steels - Internal report IM-3566”, Swedish Institute for Metals Research, Stockholm, Sweden (1998).

[2000, Craven] A. Craven, Complex heterogeneous precipitation in titanium–niobium microalloyed Al-killed HSLA steels—I. (Ti,Nb)(C,N) particles. *Acta Mater.* **48**, 3857–3868 (2000).

[2000, Wang] C.-P. Wang *et al.*, Phase equilibria in the Cu-Fe-Mo and Cu-Fe-Nb systems. *J. Phase Equilibria*. **21**, 54–62 (2000).

[2001, Dupin] N. Dupin, B. Sundman, A thermodynamic database for Ni-base superalloys, Scand. J. Metall., 30, 184-192 (2001).

[2001, Kruse] O. Kruse, B. Jansson, K. Frisk, Experimental Study of Invariant Equilibria in the Co-W-C and Co-W-C-Me (Me = Ti, Ta, Nb) Systems. *J. Phase Equilibria*. **22**, 552–555 (2001).

[2002, García de Andrés] C. García de Andrés, F. G. Caballero, C. Capdevila, L. F. Álvarez, Application of dilatometric analysis to the study of solid–solid phase transformations in steels. *Mater. Charact.* **48**, 101–111 (2002).

[2003, Coelho] G. C. Coelho, J. A. Golczewski, H. F. Fischmeister, Thermodynamic calculations for Nb-containing high-speed steels and white-cast-iron alloys. *Metall. Mater. Trans. A*. **34**, 1749–1758 (2003).

[2004a, Bratberg] J. Bratberg, K. Frisk, An Experimental Investigation of Carbide/Austenite Equilibria in *Proceeding of the Powder Metallurgy World Congress and EURO-PM2004 - Volume 5* (European Powder Metallurgy Association (EPMA), Vienna, Austria), p. 6 (2004).

[2004b, Bratberg] J. Bratberg, K. Frisk, An experimental and theoretical analysis of the phase equilibria in the Fe-Cr-V-C system. *Metall. Mater. Trans. A*. **35**, 3649–3663 (2004).

[2004, Kurokawa] H. Kurokawa, K. Kawamura, T. Maruyama, Oxidation behavior of Fe–16Cr alloy interconnect for SOFC under hydrogen potential gradient. *Solid State Ionics*. **168**, 13–21 (2004).

[2004, Sahlaoui] H. Sahlaoui, K. Makhlouf, H. Sidhom, J. Philibert, Effects of ageing conditions on the precipitates evolution, chromium depletion and intergranular corrosion susceptibility of AISI 316L: experimental and modeling results. *Mater. Sci. Eng. A*. **372**, 98–108 (2004).

[2005, Bratberg] J. Bratberg, Investigation and modification of carbide sub-systems in the multicomponent Fe–C–Co–Cr–Mo–Si–V–W system. *Zeitschrift fur Met.* **96**, 335–344 (2005).

[2005, Trindade] V. B. Trindade, U. Krupp, H.-J. Christ, M. J. Monteiro, F. C. Rizzo, Experimental Characterization and Computer-Based Simulation of Thermodynamics and Kinetics of Corrosion of Steels at High Temperatures. *Materwiss. Werksttech.* **36**, 471–476 (2005).

[2005, Sato] Y. Sato, K. Sugisawa, D. Aoki, and T. Yamamura, “Viscosities of Fe–Ni, Fe–Co and Ni–Co binary melts,” *Meas. Sci. Technol.*, **16** (2), 363 (2005).

[2006, Bratberg] J. Bratberg, B. Jansson, Thermodynamic evaluation of the C−Co−W−Hf−Zr system for cemented carbides applications. *J. Phase Equilibria Diffus.* **27**, 213–219 (2006).

[2005, Su] X. Su, J. Tedenac, Thermodynamic modeling of the ternary Ce–Fe–Sb system: Assessment of the Ce–Sb and Ce–Fe systems. *Calphad*. **30**, 455–460 (2006).

[2007, Fourmentin] R. Fourmentin, M.-N. Avettand-Fènoël, G. Reumont, P. Perrot, Optimization of the Al–Cr–Zn system at 460 °C. *J. Mater. Sci.* **42**, 7934–7938 (2007).

[2007, Lukas] H. L. Lukas, S. G. Fries, B. Sundman, *Computational Thermodynamics: the Calphad Method*, Cambridge University Press, Cambridge, UK (2007).

[2007, Miyamoto] G. Miyamoto, J. Oh, K. Hono, T. Furuhara, T. Maki, Effect of partitioning of Mn and Si on the growth kinetics of cementite in tempered Fe–0.6 mass% C martensite. *Acta Mater.* **55**, 5027–5038 (2007).

[2007, Nakano] J. Nakano, D. V Malakhov, S. Yamaguchi, G. R. Purdy, A full thermodynamic optimization of the Zn–Fe–Al system within the 420–500 °C temperature range. *Calphad*. **31**, 125–140 (2007).

[2008, Yoshitomi] K. Yoshitomi, Y. Nakama, H. Ohtani, M. Hasebe, Thermodynamic Analysis of the Fe–Nb–B Ternary System. *ISIJ Int.* **48**, 835–844 (2008).

[2008, Zhang] L. Zhang *et al.*, Thermodynamic description of the C-Fe-Mn system with key experiments and its practical applications. *Int. J. Mater. Res.* **99**, 1306–1318 (2008).

[2009, Kjellqvist] L. Kjellqvist, "Thermodynamic description of the Fe-C-Cr-Mn-Ni-O system," KTH Royal Institute of Technology, Stockholm, Sweden, (2009).

[2010, Panait] C. G. Panait, W. Bendick, A. Fuchsmann, A.-F. Gourgues-Lorenzon, J. Besson, Study of the microstructure of the Grade 91 steel after more than 100,000 h of creep exposure at 600 °C. *Int. J. Press. Vessel. Pip.* **87**, 326–335 (2010).

[2011, Djurovic] D. Djurovic, B. Hallstedt, J. von Appen, R. Dronskowski, Thermodynamic assessment of the Fe–Mn–C system. *Calphad*. **35**, 479–491 (2011).

[2011, Peng] Y. Peng *et al.*, Thermodynamic modeling of the C–RE (RE=La, Ce and Pr) systems. *Calphad*. **35**, 533–541 (2011).

[2011, Sato] Y. Sato, "Representation of the viscosity of molten alloy as a function of the composition and temperature," *Jpn. J. Appl. Phys.*, **50**, no. 11 PART 2 (2011).

[2012, Stormvinter] A. Stormvinter, A. Borgenstam, J. Ågren, Thermodynamically Based Prediction of the Martensite Start Temperature for Commercial Steels. *Metall. Mater. Trans. A*. **43**, 3870–3879 (2012).

[2013, Kobatake] H. Kobatake and J. Brillo, "Density and viscosity of ternary Cr–Fe–Ni liquid alloys," *J. Mater. Sci.*, **48**(19), 6818–6824 (2013).

[2013a, Khvan] A. V. Khvan, B. Hallstedt, Thermodynamic assessment of Fe-Mn-Nb-N and Nb-C-N systems. *Calphad*. **40**, 10–15 (2013).

[2013b, Khvan] A. V. Khvan, K. Chang, B. Hallstedt, Thermodynamic assessment of the Fe–Nb–V system. *Calphad*. **43**, 143–148 (2013).

[2013, Poletti] M. G. Poletti, L. Battezzati, Assessment of the ternary Fe–Si–B phase diagram. *Calphad*. **43**, 40–47 (2013).

[2014a, Miettinen] J. Miettinen, G. Vassilev, Thermodynamic Description of Ternary Fe-X-P Systems. Part 1: Fe-Cr-P. *J. Phase Equilibria Diffus.* **35**, 458–468 (2014).

[2014b, Miettinen] J. Miettinen, G. Vassilev, Thermodynamic Description of Ternary Fe-X-P Systems. Part 3: Fe-Mn-P. *J. Phase Equilibria Diffus.* **35**, 587–594 (2014).

[2015, Kim] S.-H. Kim, H. Kim, N. J. Kim, Brittle intermetallic compound makes ultrastrong low-density steel with large ductility. *Nature*. **518**, 77–79 (2015).

[2015, Miettinen] J. Miettinen, G. Vassilev, Thermodynamic Description of Ternary Fe-X-P Systems. Part 6: Fe-Ni-P. *J. Phase Equilibria Diffus.* **36**, 78–87 (2015).

[2015, Moon] S. C. Moon, The peritectic phase transition and continuous casting practice, Thesis, University of Wollongong, 2015.

[2016, Dilner] D. Dilner, Thermodynamic description of the Fe–Mn–Ca–Mg–S system. *Calphad*. **53**, 55–61 (2016).

[2016, Presoly] P. Presoly, J. Six, and C. Bernhard, Thermodynamic optimization of individual steel database by means of systematic DSC measurements according the CALPHAD approach., IOP Conference Series: Materials Science and Engineering. Vol. 119. No. 1. IOP Publishing, 2016.

[2016, Zhao] C. Zhao, R. Song, L. Zhang, F. Yang, T. Kang, Effect of annealing temperature on the microstructure and tensile properties of Fe–10Mn–10Al–0.7C low-density steel. *Mater. Des.* **91**, 348–360 (2016).

[2017, Pettersson] N. Pettersson, S. Wessman, S. Hertzman, and A. Studer, “High-temperature phase equilibria of duplex stainless steels assessed with a novel in-situ neutron scattering approach,” *Metall. Mater. Trans. A*, **48** (4), 1562–1571 (2017).

[2017, Sandvik] “Personal Communication with Sandvik.”

[2017, Uddeholm] “Personal Communication with Uddeholm.”

[2017, Zheng] W. Zheng, X. Lu, Y. He, L. Li, Thermodynamic modeling of Fe-C-Mn-Si alloys. *J. Iron Steel Res. Int.* **24**, 190–197 (2017).

[2018, Kobatake] H. Kobatake and J. Brillo, “Surface tension and viscosity measurement of ternary Cr-Fe-Ni liquid alloys measured under microgravity during parabolic flights.,” *High Temp. Press.*, **47** (6) (2018).

Also see our website for additional general citations using the TCFE database.

Included Phases in TCFE10

The DICTRA_FCC_A1 phases are always rejected by default. It can be restored in the TDB Module (in Console Mode) if it is necessary for your system.

Name	Prototype	Pearson	Spacegroup	Strukturbericht	SG#	CEF Fomula unit
A_R2O3_D52	A-La2O3	hP5	P-3m1	D52	164	(CE+3 CE+2)2(O-2)2(O-2 VA)1
A_YZN2	*	structure unknown				(Y)0.33(ZN)0.67
A1_FCC	Cu	cF4	Fm-3m	A1	225	(AL CA CE CO CR CU FE MG MN MO NB NI P RU S SI TA TI V W Y ZN ZR)1(VA)1
A2_BCC	W	cI2	Im-3m	A2	229	(AL CA CE CO CR CU FE MG MN MO NB NI P RU S SI TA TI V W Y ZN ZR)1(B C N O VA)3
AF	FeGaO3	oP40	Pna21		33	(AL2O3)1(FE2O3)1
AL11CE3	CdMg3	hP8	P6_3/mmc			(AL)0.79(CE)0.21
AL12MG17_A12	Mg17Al12	cI58	I-43m	A12	217	(MG)10(AL MG ZN)24(AL MG ZN)24
AL13FE4	Al13Fe4	mC102	C2/m		12	(AL)0.63(FE MN ZN)0.23(AL VA ZN)0.14
AL2CE_C15	Cu2Mg	cF24	Fd-3m	C15	227	(AL)0.67(CE)0.33
AL2CR3	MoSi2	tI6	I4/mmm		139	(AL)0.4(CR)0.5(CR ZN)0.1
AL2FE	Al2Fe	aP18	P1		1	(AL)2(FE MN)1(VA ZN)0.04
AL2S3	Al2S3	hP30	P61		169	(AL2S3)
AL2TIO5	Al2TiO5	oC32	Cmcm		63	(AL+3)2(TI+4)1(O-2)5
AL2Y_C15	Cu2Mg	cF24	Fd-3m	C15	227	(AL Y)2(AL Y)1
AL2Y3	Al2Zr3	tP20	P4_2/mnm		136	(AL)2(Y)3
AL3CE_D019	CdMg3	hP8	P6_3/mmc	D019	194	(AL)0.75(CE)0.25

Name	Prototype	Pearson	Spacegroup	Strukturbericht	SG#	CEF Fomula unit
AL3CE_L12	AuCu3	cP4	Pm-3m	L12	221	(AL)0.75(CE)0.25
AL3NB_D022	Al3Ti	tI8	I4/mmm	D022	139	(AL)3(NB)1
AL3Y_HT	BaY3	hR36	R-3m		166	(AL)0.75(Y)0.25
AL3Y_LT	Mg3Cd	hP8	P6_3/mmc		194	(AL)0.75(Y)0.25
AL4C3_D71	Al4C3	hR21	R-3m	D71	166	(AL SI)4(C)3
AL4CE_D13	BaAl4	tI10	I4/mmm	D13	139	(AL)0.8(CE)0.2
AL5FE2	Al2.8Fe	oS24	Cmcm		63	(AL)5(FE MN)2(VA ZN)3
AL5FE4	Cu5Zn8	cI52	I-43m		217	(AL FE)
AL7CR	Al45V7	mC104	C2/m		12	(AL)6(CR)1(AL ZN)1
AL8MN5_D810	Al8Cr5	hR26	R3m	D810	160	(AL)12(MN)5(AL FE MN)9
ALCE1	AlCe	oC16	Cmcm		63	(AL)0.5(CE)0.5
ALCE2_C15	Cu2Mg	cF24	Fd-3m	C15	227	(AL)0.33(CE)0.67
ALCE3_D019	CdMg3	hP8	P6_3/mmc	D019	194	(AL)0.25(CE)0.75
ALCE3_L12	AuCu3	cP4	Pm-3m	L12	221	(AL)0.25(CE)0.75
ALCRZN_TAU4	*	*	R-3m		166	(AL ZN)0.48(CR)0.12(ZN)0.4
ALMG_BETA	Al45Mg28	cF1832	Fd-3m		227	(AL ZN)89(MG)
ALMG_EPS	Al30Mg23	hR53	R-3		148	(AL ZN)30(MG)23
ALMGZN_PHI	Mg21(Al,Zn)17	oP152	Pbcm		57	(MG)21(AL ZN)17
ALMGZN_Q	*	Quasicrystal				(AL)0.15(MG)0.44(ZN)0.41
ALMGZN_T1	Mg32(Al,Zn)48	cI160	Im-3		204	(MG)26(MG AL)6(AL MG ZN)48(AL)1
ALMGZN_T2	(itself)	cP640?	Pa-3		205	(AL)0.15(MG)0.43(ZN)0.42
ALN_B4	ZnO	hP4	P6_3mc	B4	186	(AL)1(N)1
ALPHA_SPINEL	Mn3O4	tI28	I4_1/amd		141	(MG+2 MN+2 MN+3 NI+2)1(AL+3 CR+3 FE+3

Name	Prototype	Pearson	Spacegroup	Strukturbericht	SG#	CEF Fomula unit
						MN+2 MN+3 VA)2(MN+2 VA)2(O-2)4
ALY_B33	CrB	oC8	Cmcm	B33	63	(AL)1(Y)1
ALY2_C37	Co2Si	oP12	Pnma		62	(AL)1(Y)2
ANDALUSITE	Al2(SiO4)O	oP32	Pnnm		58	(AL+3)1(AL+3)1(SI+4)1(O-2)5
ANORTHITE	Ca(Al0..5Si0.5)4O8	aP52/aP104	P-1		2	(CA+2)1(AL+3)2(SI+4)2(O-2)8
B_YZN2	*	structure unknown				(Y)0.33(ZN)0.67
B3SI_D1G	B4C	hR15	R-3m	D1G	166	(B)6(SI)2(B SI)6
B4C_D1G	B13C2	hR15	R-3m	D1G	166	(B11C B12)1(B2 C2B CB2)1
BCC_A2	W	cI2	Im-3m	A2	229	(AL CA CE CO CR CU FE MG MN MO NB NI P RU S SI TA TI V W Y ZN ZR)1(B C N O VA)3
BCC_B2	CsCl	cP2	Pm-3m	B2	221	(AL CA CE CO CR CU FE MG MN MO NB NI P RU S SI TA TI V W Y ZN ZR)0.5(AL CA CE CO CR CU FE MG MN MO NB NI P RU S SI TA TI V W Y ZN ZR)0.5(B C N O VA)3
BETA_RHOMBO_B	beta-B	hR105	R-3m		166	(B)93(B C SI)12
BN_B4	BN	hP4	P6_3/mmc		194	(B1N1)
C12A7	Al14Ca12O33	cI152	I-43d		220	(CA+2)6(AL+3)6(AL+3 FE+3)1(O-2)16.5
C14_LAVES	MgZn2	hP12	P63/mmc	C14	194	(AL CO CR CU FE MG MN MO NB NI SI TA TI V W Y ZN ZR)2(AL CO CR CU FE MG MN MO NB NI SI TA TI V W Y ZN ZR)1
C15_LAVES	Cu2Mg	cF24	Fd-3m	C15	227	(CE NI)0.33(CE NI)0.67
C1A1	Al2CaO4	mP84	P2_1/c		14	(CA+2)1(AL+3)2(O-2)4
C1A2	Al4CaO7	mC48	C2/c		15	(CA+2)1(AL+3)4(O-2)7
C1A6	Fe12PbO19	hP64	P6_3/mmc		194	(CA+2)1(AL+3)12(O-2)19

Name	Prototype	Pearson	Spacegroup	Strukturbericht	SG#	CEF Fomula unit
C1A8M2	CaMg2Al16O27	hP94	P-6m2		187	(CAO)1(AL2O3)8(MGO)2
C2A14M2	*	hR114	R-3m:h		166	(CAO)2(AL2O3)14(MGO)2
C2F	Ca2Fe2O5	oP36	Pnma		62	(CA+2)2(FE+3)2(O-2)5
C3A1	Ca3Al2O6	cP264	Pa-3		205	(CA+2)3(AL+3)2(O-2)6
C3A2M1	*	o??	Pbcm		57	(CAO)3(AL2O3)2(MGO)1
C4WF4	Ca4Fe9O17	mS60	C2		5	(CA+2)4(FE+2)1(FE+3)8(O-2)17
C4WF8	Sr2Fe2O5	oI44	Imma		74	(CA+2)4(FE+2)1(FE+3)16(O-2)29
CA1CR2O4_A	SrCr2O4	oP28	Pmmn		59	(CA1CR2O4)
CA1CR2O4_B	CaV2O4	oP28	Pnma		62	(CA1CR2O4)
CA2NI7	Co7Gd2	hR18	R-3m		166	(CA)2(NI)7
CA2SIO4_ALPHA	Ca2SiO4	hP24	P6_3/mmc		194	(CA+2 MG+2)2(SI+4)1(O-2)4
CA2SIO4_ALPHAP	K2CoCl4	oP84	Pna21		33	(CA+2 FE+2 MG+2)2(SI+4)1(O-2)4
CA3ZN_E1A	Re3B	oC16	Cmcm	E1A	63	(CA)3(ZN)1
CA5ZN3_D8L	Cr5B3	tI32	I4/mcm	D8L	140	(CA)5(ZN)3
CAMN2O4	CaMn2O4	oP28	Pbcm		57	(CA+2)1(MN+3)2(O-2)4
CAMNO3	GdFeO3/CaTiO3	oP20/cP5	Pnma / Pm-3m		62/221	(CA+2)1(MN+4)1(O-2)3
CANI2_C15	Cu2Mg	cF24	Fd-3m	C15	227	(NI)2(CA)1
CANI3	Ni3Pu	hR12	R-3m		166	(CA)0.25(NI)0.75
CANI5_D2D	CaCu5	hP6	p&/mmm	D2D	191	(CA)1(NI)5
CAZN_B33	CrB	oC8	Cmcm	B33	63	(ZN)1(CA)1
CAZN11	BaCd11	tI48	I4_1/amd		141	(CA)1(ZN)11
CAZN13_D23	NaZn13	cF112	Fm-3c	D23	226	(CA)1(ZN)13
CAZN2	Hg2K	oI12	Imma		74	(ZN)2(CA)1

Name	Prototype	Pearson	Spacegroup	Strukturbericht	SG#	CEF Fomula unit
CAZN3	CaZn3	hP32	P6_3/mmc		194	(CA)1(ZN)3
CAZN5_D2D	CaCu5	hP6	P6/mmm	D2D	191	(CA)1(ZN)5
CBCC_A12	alpha-Mn	cI58	I-43m	A12	217	(AL CO CR CU FE MG MN MO NB NI P RU SI TA TI V ZN ZR)1(B C N VA)1
CE13ZN58	Gd13Zn58	hP142	P6_3/mmc		194	(CE)0.18(ZN)0.82
CE1N1	NaCl	cF8	Fm-3m		225	(CE)1(N)1
CE1S1	NaCl	cF8	Fm-3m		225	(CE)1(S)1
CE1S2	Ce10Se19	tP58	P42/n		86	(CE)1(S)2
CE24CO11	Ce24Co11	hP70	P6_3mc		186	(CO)11(CE)24
CE2C3_D5C	Pu2C3	cI40	I-43d	D5C	220	(CE)0.4(C)0.6
CE2CO7	Ce2Ni7/Co7Gd2	hP36/hR18	P6_3/mmc / R-3m		194/166	(CO)7(CE)2
CE2FE17	Ni17Th2	hP38	P6_3/mmc		194	(CE)2(FE)17
CE2NI7	Ce2Ni7	hP36	P6_3/mmc		194	(CE)0.22(NI)0.78
CE2O12S3	*	m**	P2_1/c / P6_3/m		14/176	(CE)2(O)12(S)3
CE2O2S1	Ce2SO2	hP5	P-3m1		164	(CE)2(O)2(S)1
CE2O3_D53	Mn2O3	cI180	Ia-3	D53	206	(CE+3 CE+4)2(O-2 VA)3(O-2 VA)1
CE2S3	Th3P4/Cr3C2-b	cI28/oP20	I-43d/Pnma	D73/D510	220/62	(CE)2(S)3
CE2ZN17	Ni17Th2	hP38	P6_3/mmc		194	(CE)0.1(ZN)0.9
CE3S4_D73	Th3P4	cI28	I-43d	D73	220	(CE)3(S)4
CE3ZN11	Al11La3	oI28	Immm		71	(CE)0.21(ZN)0.79
CE3ZN22	Ce3Zn22	tI100	I4_1/amd		141	(CE)0.12(ZN)0.88
CE5CO19	Ce5Co19	hR24	R-3m		166	(CO)19(CE)5

Name	Prototype	Pearson	Spacegroup	Strukturbericht	SG#	CEF Fomula unit
CE7NI3_D102	Fe3Th7	hP20	P6_3mc	D102	186	(CE)0.7(NI)0.3
CE7O12	Pr7O12	hR19	R-3		148	(CE)7(O)12
CEB4_D1E	UB4	tP20	P4/mbm	D1E	127	(B)0.8(CE)0.2
CEB6_D21	CaB6	cP7	Pm-3m	D21	221	(B)0.86(CE)0.14
CEC2_BETA	CaC2	cF36	Fm-3m		225	(CE)0.33(C)0.67
CEC2_C11A	CaC2	tI6	I4/mmm	C11A	139	(CE)0.33(C)0.67
CECO2_C15	Cu2Mg	cF24	Fd-3m	C15	227	(CO)2(CE)1
CECO3	Ni3Pu	hR12	R-3m		166	(CO)3(CE)1
CECO5_D2D	CaCu5	hP6	P6/mmm	D2D	191	(CO)5(CE)1
CECU_B27	FeB	oP8	Pnma	B27	62	(CU)0.5(CE)0.5
CECU2	Hg2K	oI12	Imma		74	(CU)0.67(CE)0.33
CECU4	CeCu4	oP20	Pnnm		58	(CU)0.8(CE)0.2
CECU5_D2D	CaCu5	hP6	P6/mmm	D2D	191	(CU)0.83(CE)0.17
CECU6	CeCu6	oP28	Pnma		62	(CU)0.86(CE)0.14
CEFE2_C15	Cu2Mg	cF24	Fd-3m	C15	227	(FE)2(CE)1
CEMENTITE_ D011	Fe3C	oP16	Pnma	D011	62	(AL CO CR FE MN MO NB NI SI V W)3(B C N)1
CENI_B33	CrB	oC8	Cmcm	B33	63	(CE)0.5(NI)0.5
CENI3	CeNi3	hP24	P6_3/mmc		194	(CE)0.25(NI)0.75
CENI5_D2D	CaCu5	hP6	P6/mmm	D2D	191	(CE NI)1(CE NI)5
CESI2_CC	Si2Th	tI12	I4_1/amd	CC	141	(CE)0.33(SI)0.67
CEZN_B2	CsCl	cP2	Pm-3m	B2	221	(CE)0.5(ZN)0.5
CEZN11	BaCd11	tI48	I4_1/amd		141	(CE)0.08(ZN)0.92

Name	Prototype	Pearson	Spacegroup	Strukturbericht	SG#	CEF Fomula unit
CEZN2	Hg2K	oI12	Imma		74	(CE)0.33(ZN)0.67
CEZN3	CeZn3	oC16	Cmcm		63	(CE)0.25(ZN)0.75
CEZN5_D2D	CaCu5	hP6	P6/mmm	D2D	191	(CE)0.17(ZN)0.83
CF1	CaV2O4	oP28	Pnma		62	(CA+2)1(FE+3)2(O-2)4
CF2	Ca3.5Fe14O24.5	mS172	C2		5	(CA+2)1(FE+3)4(O-2)7
CHI_A12	a-Mn	cI58	I-43m	A12	217	(CR FE NI)24(CR MO W ZR)10(CR FE MO NI W)24
CLINO_ PYROXENE	CaMgSi2O6	MS40	C2/c		15	(CA+2 FE+2 MG+2)1(FE+2 MG+2)1(SI+4)2(O-2)6
CO17Y2	Th2Zn17/Ni17Th2	hR19/hP38	R-3m/P6_ 3/mmc		166/191	(CO2 Y)1(CO2 Y)2(CO)15
CO2SI_C37	Co2Si	oP12	Pnma		62	(FE NI)2(SI)1
CO2ZN15_ GAMMA1	Zn7.8Co	mS28	C2m:b1		12	(CO)0.12(ZN)0.88
CO3MO_D019	CdMg3	hP8	P6_3/mmc	D019	194	(CO)3(MO)1
CO3V	Al3Pu	hP24	P6_3/mmc		194	(CO V)3(CO V)1
CO3Y	Ni3Pu	hR12	R-3m		166	(CO)3(Y)1
CO3Y2	*	cP*	*			(CO)3(Y)2
CO3Y4	Co3Ho4	hP22	P6_3/m		176	(CO)3(Y)4
CO5Y_D2D	CaCu5	hP6	P6/mmm	D2D	191	(CO2 Y)1(CO)4(CO VA)1
CO5Y8	Co5Y8	mP52	P2_1/c		14	(CO)5(Y)8
CO7Y6	*	structure unknown				(CO)7(Y)6
CO9S8	Co9S8	cF68	Fm-3m		225	(CO FE)9(S)8
COP1	FeAs	oP8	Pnma		62	(CO)1(P)1

Name	Prototype	Pearson	Spacegroup	Strukturbericht	SG#	CEF Fomula unit
COP3	cI32	cI32	Im-3		204	(CO)1(P)3
CORDIERITE	Na0.04 (Mg0.5Fe0.5)2Al4Si5O18	oS120	Cccm		66	(AL4MG2O18SI5)
CORUNDUM	Al2O3	hR30	R-3c	D51	167	(AL+3 CR+2 CR+3 FE+2 FE+3 MN+3 TI+3)2(CR+3 FE+3 NI+2 VA)1(O-2)3
COY_B33	CrB	oC8	Cmcm	B33	63	(CO)1(Y)1
COZN_A13	beta-Mn	cP20	P4_132	A13	213	(CO ZN)1(CO ZN)1
COZN13	Zn13Co	mS28	C2m:b1		12	(CO)0.07(ZN)0.93
COZN4_D83	Zn9(Zn0.5Fe0.5)2Fe2	cI52	I-43m	D83	217	(CO ZN)4(CO ZN)1
CR3RU_A15	Cr3Si	cP8	Pm-3n	A15	223	(CR)0.69(RU)0.32
CR3SI_A15	Cr3Si	cP8	Pm-3n	A15	223	(CO CR FE MO NB SI V)3(AL CO CR NB SI V)1
CR5B3_D8L	CR5B3	tI32	I4/mcm	D8L	140	(CR MO)0.62(B)0.38
CR5SI3_D8M	W5Si3	tI32	I4/mcm	D8m	140	(CR)4(CR)1(SI)3
CRISTOBALITE	SiO2	tP12/cF24	P4_12_12 / Fd-3m	*/C9	92/227	(SIO2)
CRNBSI	ZrNiAl	hP9	P-62m		189	(CR)1(NB)1(SI)1
CRZN17	*	hP*	*			(AL CR)1(FE ZN)17
CU2S_ALPHA	Cu2S	mP144	P121/c1		14	(CU)2(S)1
CU2S_BETA	Cu2S	hP16	P63/mmc		194	(CU)2(S)1
CU2S_GAMMA	Cu2Se	cF44	Fm-3m		225	(CU FE VA)2(CU VA)1(S)1
CU2Y_H	*	hP*	*			(CU)2(Y)1
CU2Y_L	Hg2K	oI12	Imma		74	(CU)2(Y)1
CU31S16	Cu31S16	mP376	P2_1/c:a3		14	(CU)1.93(S)1
CU3P_D021	Cu3P	P3c1	hp24	D021	185	(CU FE)3(P)1

Name	Prototype	Pearson	Spacegroup	Strukturbericht	SG#	CEF Fomula unit
CU4Y	Cu5Y1.25	mP16	P21/m:a		11	(CU)4(Y)1
CU6Y	Cu7Tb	hP8	P6/mmm		191	(CU2 Y)1(CU)5
CU7S4	Cu7S4	oP44	Pnma		62	(CU)1.75(S)1
CU7Y2	Ag51Gd14	hP68	P6/m		175	(CU)7(Y)2
CUB_A13	beta-Mn	cP20	P4_132	A13	213	(AL CE CO CR CU FE MG MN MO NB NI P RU SI TA TI V Y ZN ZR)1(B C N VA)1
CUO_B26	CuO	mS8	C2/c	B26	15	(CU+2)1(O-2)1
CUPRITE_C3	Cu2O	cP6	Pn-3m	C3	224	(CU+1)2(O-2)1
CUS_B18	CuS-b	hP12	P63/mmc	B18	194	(CU)1(S)1
CUZN_EPSILON	Mg	hP2	P6_3/mmc	A3	194	(CU MN ZN)1(VA)0.5
CUZR_B2	CsCl	cP2	Pm-3m	B2	221	(CU)1(Y)1
CW3F	CaFe5O7	oS52	Cmcm		63	(CA+2)1(FE+2)3(FE+3)2(O-2)7
CWF	CaFe3O5	oS36	Cmcm		63	(CA+2)1(FE+2)1(FE+3)2(O-2)5
DIAMOND_A4	C	cF8	Fd-3m	A4	227	(AL B C MN O P SI ZN)
DICTRA_FCC_A1	Cu	cF4	Fm-3m	A1	225	(AL CA CE CO CR CU FE MG MN MO NB NI P RU S SI TA TI V W Y ZN ZR)1(B C N O VA)1
ETA_M5SIN	Cr3Ni2SiN	cF112	Fd-3m		227	(CR MO)3(NI FE)2(SI)1(N)1
F_CEO2	CaF2	cF12	Fm-3m	C1	225	(CE+3 CE+4)2(O-2 VA)4
FCC_A1	Cu	cF4	Fm-3m	A1	225	(AL CA CE CO CR CU FE MG MN MO NB NI P RU S SI TA TI V W Y ZN ZR)1(B C N O VA)1
FCC_L12	AuCu3	cP4	Pm-3m	L12	221	(AL CA CE CO CR CU FE MG MN MO NB NI P RU S SI TA TI V W Y ZN ZR)0.75(AL CA CE CO CR CU FE MG MN MO NB NI P RU S SI TA TI V W Y ZN ZR)0.25(VA)1
FE10SI2B3	*	structure unknown				(FE)2(SI)0.4(B)0.6

Name	Prototype	Pearson	Spacegroup	Strukturbericht	SG#	CEF Fomula unit
FE1NB1B1_C22	Fe2P	hP9	P26m	C22	189	(FE)0.33(NB)0.33(B)0.33
FE2S3O12	Fe2(SO4)3	mP68/hR102	P2_1/c / R-3		14/148	(FE)2(S)3(O)12
FE2SITI_L21	BiF3	cF16	Fm-3m	D03	225	(FE)0.5(SI)0.25(TI)0.25
FE3NB3B4	*	structure unknown				(FE)0.3(NB)0.3(B)0.4
FE3NB4SI5	Nb12Fe7 (Fe0.5Si0.5)5Si12	oP72	Pmn21		31	(FE)3(NB)4(SI)5
FE3ZN7_D82	Cu5Zn8	cI52	I-43m	D82	217	(FE ZN)0.15(FE ZN)0.15(AL FE ZN)0.23(ZN)0.46
FE4N_LP1	Fe4N	cP5	Pm-3m	L'1	221	(CO CR FE MN NI)4(C N)1
FE4NB2O9	Nb2Mn4O9	hP30	P-3c1		165	(FE+3)4(NB+2)1(NB+4)1(O-2)9
FE4NB4SI7	Zr4Co4Ge7	tI60	I4/mmm		139	(FE)4(NB)4(SI)7
FE5SI2B	Nb5Sn2Si	tI32	I4/mcm		140	(FE)4.7(SI)2(B)1
FE5SIB2	Mo5SiB2	tI32	I4/mcm		140	(FE)5(SI)1(B)2
FE8SI2C	Mn8Si2C3	aP*	P1			(FE MN)8(SI)2(C)1
FEAL2S4	ZnIn2S4	hR21	R3m		160	(FE)1(AL)2(S)4
FECN_CHI	Mn5C2	mS28	C2/c		15	(FE)2.2(C N)1
FENB2P	Cu3Au	cP4	Pm-3m		221	(FE)1(NB)2(P)1
FENB2SI2	Nb39Fe20Si40	tP198	P42/mcm		132	(FE)1(NB)2(SI)2
FENB4P	Nb4CoSi	tP12	P4/mcc		124	(FE)1(NB)4(P)1
FENB4SI	Nb4CoSi	tP12	P4/mcc		124	(FE)1(NB)4(SI)1
FENBSI	TiNiSi	oP12	Pnma		62	(FE)1(NB)1(SI)1
FENBSI2	ZrCrSi2	oP48	Pbam		55	(FE)1(NB)1(SI)2
FESI2_H	FeSi2-h	oC48	Cmca		64	(FE)0.3(SI)0.7

Name	Prototype	Pearson	Spacegroup	Strukturbericht	SG#	CEF Fomula unit
FESI2_L	FeSi2-l	tP3	P4/mmm		123	(FE)0.33(SI)0.67
FESI4P4	FeSi4P4	aP9	P1		1	(FE)1(SI)4(P)4
FESO4	CuSO4	oP24	Pnma		62	(FE)1(S)1(O)4
FETIP_C37	NiSiTi	oP12	Pnma	C37	62	(FE)1(TI)1(P)1
FEWB_C37	NiSiTi	oP12	Pnma	C37	62	(FE)1(W)1(B)1
FEZN10	FeZn10	hP632	P6_3/mmc		194	(CR FE)0.06(AL FE ZN)0.18(ZN)0.53(ZN)0.24
FEZN13	CoZn13	mC28	C2/m		12	(CR FE VA)0.07(AL ZN VA)0.07(AL ZN)0.86
FEZN4	Fe11Zn40	cF408	F-43m		216	(FE)0.14(AL FE ZN)0.12(ZN)0.74
FLUORITE_C1	CaF2	cF12	Fm-3m	C1	225	(MN+2 MN+3 NI+2 Y+3 ZR ZR+4)2(O-2 VA)4
G_PHASE	Mn23Th6	cF116	Fm-3m	D8A	225	(AL CO FE NI TI)16(MN NB TI Y ZR)6(CO FE NI SI)7
GAMMA_D82	Cu5Zn8	cI52	I-43m	D82		(ZN)4(CU ZN)1(CU ZN)8
GAMMA2_ ALFEZN	*	structure unknown				(AL FE ZN)0.26(ZN)0.74
GAS						(AR C C1H1 C1H1N1O1 C1H1N1_HCN C1H1N1_ HNC C1H1O1 C1H1O2 C1H2 C1H2O1 C1H2O2_ CIS C1H2O2_DIOXIRANE C1H2O2_TRANS C1H3 C1H3O1_CH2OH C1H3O1_CH3O C1H4 C1H4O1 C1N1 C1N1O1 C1N1O1_NCO C1N2_CNN C1N2_NCN C1O1 C1O1S1 C1O2 C1S1 C1S2 C2 C2H1 C2H1N1 C2H2 C2H2O1 C2H3 C2H4 C2H4O1_ACETALDEHYDE C2H4O1_OXIRANE C2H4O2_ACETICACID C2H4O2_DIOXETANE C2H4O3_123TRIOXOLANE C2H4O3_ 124TRIOXOLANE C2H5 C2H6 C2H6O1 C2H6O2 C2N1_CCN C2N1_CNC C2N2 C2O1 C3 C3H1 C3H1N1 C3H4_1 C3H4_2 C3H6 C3H6O1 C3H6_2 C3H8 C3N1 C3O2 C4 C4H1 C4H10_1 C4H10_2 C4H2 C4H4 C4H4_1_3 C4H6_1 C4H6_2 C4H6_3 C4H6_4 C4H6_5 C4H8 C4H8_1 C4H8_2 C4H8_3

Name	Prototype	Pearson	Spacegroup	Strukturbericht	SG#	CEF Fomula unit
						C4H8_4 C4H8_5 C4N1 C4N2 C5 C5H1N1 C5N1 C60 C6H6 C6H6O1 C6N1 C6N2 C9N1 H H1N1 H1N1O1 H1N1O2_CIS H1N1O2_TRANS H1N1O3 H1N3 H1O1 H1O1S1_HSO H1O1S1_SOH H1O2 H1S1 H2 H2N1 H2N2O2 H2N2_1_1N2H2 H2N2_CIS H2N2_TRANS H2O1 H2O1S1_H2SO H2O1S1_HSOH H2O2 H2O4S1 H2S1 H2S2 H3N1 H3N1O1 H4N2 N N1O1 N1O2 N1O3 N1S1 N2 N2O1 N2O3 N2O4 N2O5 N3 O O1S1 O1S2 O1Y1 O1Y2 O2 O2S1 O2Y1 O2Y2 O3 O3S1 S S2 S3 S4 S5 S6 S7 S8 V Y ZN ZR ZR2)
GRAPHITE_A9	C	hP4	P6_3/mmc	A9	194	(B C)
H_R2O3	H-La2O3	hP10	P6_3/mmc		194	(CE+2 CE+3)2(O-2)2(O-2 VA)1
HALITE	NaCl	cF8	Fm-3m	B1	225	(AL+3 CA+2 CR+3 FE+2 FE+3 MG+2 MN+2 MN+3 NI+2 NI+3 SI+4 VA)1(O-2)1
HATRURITE	Ca3(SiO4)O-b	hR81	R3m		160	(CA+2)3(SI+4)1(O-2)5
HCP_A3	Mg	hP2	P6_3/mmc	A3	194	(AL CA CE CO CR CU FE MG MN MO NB NI P RU S SI TA TI V W Y ZN ZR)1(B C N O VA)0.5
HIGH_SIGMA	CrFe	tP30	P4_2/mnm		136	(MN)8(CR)4(CR MN)18
K_PHASE	CaTiO3	cP5	Pm-3m	E21	221	(C CO ZN)51(ZN)32(C)17
KAPPA_E21	CaTiO3	cP5	Pm-3m	E21	221	(AL)1(FE MN)3(C VA)1
KSI_CARBIDE	Mo6Fe11C5	mS44	C12/m1		12	(CR FE MO W)3(C)1
KYANITE	Al2SiO5	aP32	P-1		2	(AL+3)1(AL+3)1(SI+4)1(O-2)5
LARNITE	CaSiO3	mP60	P2_1/n		14	(CA+2)2(SI+4)1(O-2)4
LIQUID						(AL ALN ALO3/2 AL2/3S B C CA CAS CE CEO2 CEO3/2 CO COS CR CRO3/2 CRS CU CU2O CUO CU2S FE FEO FEO3/2 FES MG MGS MN MNO MNO3/2 MNS MO MO1/2S N NB NBO NBO2 NBS NI NIO NIS P RU S S2ZR S3ZR2 SI SIO2 SI1/2S SZN TA TI TIO TIO3/2 TIO2 V W Y Y2/3O ZN ZR

Name	Prototype	Pearson	Spacegroup	Strukturbericht	SG#	CEF Fomula unit
						ZR1/2O)
LOWCLINO_ PYROXENE	CaMgSi2O6	mS40	P2_1/c		15	(CA+2 MG+2)1(MG+2)1(SI+4)2(O-2)6
M11SI8	Cr8Nb3Si8	oP76	Pnma		62	(CR NB)11(SI)8
M12C	W6Fe6C	cF104	Fd-3m		227	(CO)6(W)6(C)1
M1B6_D21	CaB6	cP7	Pm3m	D21	221	(CA Y)1(B)6
M23C6_D84	Cr23C6	cF116	Fm-3m	D84	225	(CO CR FE MN NI V)20(CO CR FE MN MO NI V W)3(B C)6
M2B_C16	Al2Cu	tI12	I4/mcm	C16	140	(CO CR FE MN MO NI V W)2(B)1
M2B_CB	Mg2Cu	oF48	Fddd	CB	70	(CR FE MO MN NI)0.67(B)0.33
M2B3	V2B3	oS20	Cmcm		63	(NB V)0.4(B)0.6
M2O3C_D53	(Mn0.5Fe0.5)2O3	cI80	Ia-3	D53	206	(AL+3 CR+3 FE+3 MN+3 NI+2 Y Y+3 ZR+4)2(O-2 VA)3(O-2 VA)1
M2O3H_D52	La2O3	hP5	P-3m1	D52	164	(MN+3 Y Y+3 ZR+4)2(O-2 VA)3(O-2 VA)1
M2P_C22	Fe2P	hP9	P-62m	C22	189	(AL CO CR FE MN MO NB NI TI W)2(P SI)1
M2P_C37	Co2P	oP12	Pnma		62	(CO FE NB W)2(P)1
M2SI_TETA	Ga3Ge6Ni13	hP66	P3_121		152	(FE NI)1(FE NI VA)1(SI)1
M3B2_D5A	Mo2FeB2	tP10	P4/mbm	D5A	127	(CR FE MO NI W)0.4(CR FE NI)0.2(B)0.4
M3B4_D7B	Ta3B4	oI14	Immm	D7B	71	(CR FE NB V)0.43(B)0.57
M3C2_D510	Cr3C2	oP20	Pnma	D510	62	(CO CR MO V W)3(C)2
M3P_D0E	Ni3P	tI32	I-4	D0E	82	(AL CO CR CU FE MN MO NI TI)3(P)1
M3SI	BiF3	cF16	Fm-3m		225	(FE MN)3(SI)1
M4SI1_G3	AlAu4	cP20	P2_13	G3	198	(CR FE NI)3(NI)1(SI)1(C VA)1
M5B6	V5B6	oS22	Cmmm		65	(V NB)0.46(B)0.55

Name	Prototype	Pearson	Spacegroup	Strukturbericht	SG#	CEF Fomula unit
M5C2	Mn5C2	mC28	C2/c		15	(FE MN NB V)5(C)2
M5SI3_D88	Mn5Si3	hP16	P6_3/mcm	D88	193	(CR FE MN NI Y)0.62(SI)0.38
M6C_E93	W3Fe3C	cF112	Fd-3m	E93	227	(CO FE NI)2(MO NB W)2(CO CR FE MO NB NI SI V W)2(C)1
M6SI5	V6Si5	oI44	Ibam		72	(CR NB)6(SI)5
M7C3_D101	Cr7C3	oP40	Pnma	D101	62	(AL CO CR FE MN MO NB NI SI V W)7(B C)3
M7Y2	Co7Gd2	hR18	R-3m		166	(CO NI)7(Y)2
MB_B27	FeB	oP8	Pbnm	B27	62	(B)1(CO CR FE MN MO NI TI V ZR)1
MB_B33	CrB	oC8	Cmcm	B33	63	(CR FE MN MO NB NI TA TI V)1(B)1
MB_BG	MoB	tI16	I4/amd	BG	141	(CR FE MO)0.5(B)0.5
MB2_C32	AlB2	hp3	P6/mmm	C32	166	(B)2(AL CR MG TI Y ZR)1
MC_ETA	MoC	hP12	P63/mmc	B_i	194	(MO TI V W)1(C VA)1
MC_SHP	WC	hP2	P-6m2	B_h	187	(MO W)1(C N)1
MELILITE	Ca2MgSi2O7	tP24	P-42_1m		113	(CA+2)2(AL+3 MG+2)1(AL+3 SI+4)1(SI+4)1(O-2)7
MERWINITE	Ca3Mg(SiO4)2	mP56	P2_1/a		14	(CA+2)3(MG+2)1(SI+4)2(O-2)8
MG12R_D2B	Mn12Th	tI26	I4/mmm	D2B	139	(MG)12(CE)1
MG12ZN13	Re25Zr21	hR92	R-3c		167	(MG)12(AL ZN)13
MG17R2	CeMg10	hP44	P6_3/mmc		194	(MG)17(CE)2
MG2C3	Mg2C3	oP10	Pnnm		58	(MG)2(C)3
MG2M_C15	Cu2Mg	cF24	Fd-3m	C15	227	(MG)2(CE)1
MG2NI_CA	Mg2Ni	hP18	P6_222	Ca	180	(MG)2(NI)1
MG2SI_C1	CaF2	cF12	Fm-3m	C1	225	(MG)2(SI)1

Name	Prototype	Pearson	Spacegroup	Strukturbericht	SG#	CEF Fomula unit
MG2ZN11_D8C	Mg2Zn11	cP39	Pm-3	D8C	200	(MG)2(AL ZN)11
MG2ZN3	Mg4Zn7	mC110	C2/m		12	(MG)2(AL ZN)3
MG3M_D03	BiF3	cF16	Fm-3m	D03	225	(MG)3(CE MG)1
MG3N2_D53	Mn2O3	cI180	Ia-3	D53	206	(MG)3(N)2
MG41M5	Ce5Mg41	tI92	I4/m		87	(MG)41(CE)5
MG51ZN20	Mg51Zn20	oI158	Immm		71	(MG)51(ZN)20
MGB4	MgB4	oP20	Pnma		62	(MG)1(B)4
MGB7	MgB7	oI64	Imma		74	(MG)1(B)7
MGC2	MgC2	tP6	P4_2/mnm		136	(MG)1(C)2
MN11SI19	Mn11Si19	tP120	P-4n2		118	(MN)0.37(SI)0.63
MN2YO5	DyMn2O5	oP32	Pbam		55	(Y+3)1(MN+3)1(MN+4)1(O-2)5
MN3N2	Mn3N2	tI10	I4/mmm		139	(MN)3(N)2
MN3P_D0E	Ni3P	tI32	I-4	D0E	82	(MN FE)3(P)1
MN5SIC	Mn5SiC	oS56	CmC2_1		36	(MN)0.71(SI)0.14(C)0.14
MN5SIC	CoO	tI4	I4/mmm		139	(MN)6(N)5
MN6SI	R-(Co,Cr,Mo)	hR53	R-3		166	(MN)0.86(SI)0.14
MN9SI2	Mn9Si2	oI186	Immm		71	(MN)0.82(SI)0.18
MNO2_C4	TiO2	tP6	P4_2/mnm	C4	136	(MN+4)1(O-2)2
MNP_B31	MnP	oP8	Pnma	B31	62	(CR FE MN W)1(P SI)1
MNTA	*	structure unknown				(MN)1(TA)1
MNYO3_HEX	LuMnO3	hP30	P6_3cm		185	(Y+3)1(MN+3)1(O-2)3
MNZN9	MnZn9?	h**	*			(MN)0.1(ZN)0.9

Name	Prototype	Pearson	Spacegroup	Strukturbericht	SG#	CEF Fomula unit
MO2B5_D8I	MO2B5	hR7	R3m	D8I	166	(MO)0.32(B)0.68
MO2S3	Mo2S3	mP10	P2_1/m		11	(MO)2(S)3
MO3P_D0E	V3S	tI32	I-42m	D0E	121	(MO)3(P)1
MO5SI3_D8M	Si3W5	tI32	I4/mcm	D8M	140	(MO)5(SI)3
MOB2_C32	AlB2	hp3	P6/mmm	C32	191	(MO)0.38(B)0.62
MOP_BH	WC	hP2	P-6m2	BH	187	(MO)1(P)1
MOS2_C7	MoS2	hP6	P6_3/mmc		194	(MO W)1(S)2
MOSI2_C11B	MoSi2	tI6	I4/mmm	C11B	139	(MO)1(SI)2
MOZN22	Zn93 (Zn0.43Mo0.57)Mo4	cF420	F-43m		216	(MO)1(ZN)22
MOZN7	CuPt7	cF32	Fm-3m		225	(MO)1(ZN)7
MS_B1	NaCl	cF8	Fm-3m	B1	225	(CA CO CR CU FE MG MN Y)1(S)1
MS_B81	NiAs	hP4	P63/mmc	B81	194	(AL CO CR CU FE MN NB NI TI V VA)1(S)1
MS2_C2	FeS2	cP12	Pa-3	C2	205	(CO FE MN)1(S)2
MSI_B20	FeSi	cP8	P213	B20	198	(CO CR FE MN NI)0.5(AL SI)0.5
MSI2_C40	CrSi2	hP9	P6_222	C40	180	(CR NB)1(SI)2
MU_D85	Fe7W6	hR13	R-3m	D85	166	(CO CR FE MN NB NI TA)7(MO NB TA W)2(CO CR FE MO NB NI TA W)4
MULLITE	Al(Al0.7Si0.3)2O4.8	oP24	Pbam		55	(AL+3)1(AL+3)1(AL+3 SI+4)1(O-2 VA)5
MY3_D011	Fe3C	oP16	Pnma	D011	62	(CO NI)1(Y)3
NB3B2_D5A	U3Si2	tP10	P4/mbm	D5A	127	(FE NB V)0.6(B)0.4
NB3RU5	*/CsCl	o**/cP2	?/Pm-3m		?/221	(NB RU)0.38(RU)0.62
NB3SI	Ti3P	tP32	P4_2/n		86	(NB)3(SI)1

Name	Prototype	Pearson	Spacegroup	Strukturbericht	SG#	CEF Fomula unit
NB5SI3_D8L	Cr5B3	tI32	I4/mcm	D8L	140	(CR NB)5(SI)3
NB5SI3_D8M	W5Si3	tI32	I4/mcm	D8M	140	(NB)4(CR NB SI)1(SI)3
NB7P4	Nb7P4	mS44	C12/m1		12	(NB)7(P)4
NBNI3_D0A	Cu3Ti	oP8	Pmmn	D0A	59	(NB NI)1(NB NI)3
NBO	NbO	cP6	Pm-3m		221	(NB+2)1(O-2)1
NBP	NbAs	tI8	I41md		109	(NB)1(P)1
NI17Y2	Fe17Lu2	hP80	P6_3/mmc		194	(FE NI)1(Y)0.12
NI2Y	Ni2Tm	cF192	F-43m		216	(NI)2(Y)1
NI2Y3	Ni2Y3	tP80	P4_12_12		92	(NI)2(Y)3
NI2ZN11_D82	Cu5Zn8	cI52	I4-3m	D82	217	(NI ZN)1(VA)1
NI31SI12	Ni31S12	hP42	P321		150	(FE NI)5(SI)2
NI3S2_LT	Ni3S2	hR15	R32		155	(NI)3(S)2
NI3SI2	Ni3Si2	oP80	Cmc2_1		36	(FE NI)3(SI)2
NI3TI_D024	Ni3Ti	hP16	P6_3/mmc	D024	194	(FE NI TI)0.75(NI TI)0.25
NI3Y	Ni3Pu	hR12	R-3m		166	(FE NI)3(Y)1
NI4Y	*	hR*	*			(NI)4(Y)1
NI5Y_D2D	CaCu5	hP6	P6/mmm	D2D	191	(NI)5(Y)1
NI6MNO8	NaCl	cF8	Fm-3m	B1?	225	(MG+2 NI+2)6(MN+4)1(O-2)8
NIMNO3	*	hR10	R-3		148	(MN+3 MN+4 NI+2)2(O-2)3
NISI_B31	MnP	oP8	Pnma		62	(FE NI)1(SI)1
NITI2	NiTi2	cF96	Fd-3m		227	(NI)0.33(TI)0.67
NIY_B27	FeB	oP8	Pnma	B27	62	(NI)1(Y)1
NIZN_B2	CsCl	cP2	Pm-3m	B2	221	(NI ZN)1(VA)1

Name	Prototype	Pearson	Spacegroup	Strukturbericht	SG#	CEF Fomula unit
NIZN_L10	AuCu	tP4	P4/mmm	L10	123	(NI ZN)1(VA)3
NIZN8	Ni3Zn22	mC50	C2/m		12	(NI)1(ZN)8
OLIVINE	Mg2SiO4	oP28	Pnma		62	(CA+2 FE+2 MG+2 MN+2 NI+2)1(CA+2 FE+2 MG+2 MN+2 NI+2)1(SI+4)1(O-2)4
ORTHO_ PYROXENE	MgSiO3	oP80	Pbca		61	(CA+2 MG+2)1(MG+2)1(SI+4)2(O-2)6
ORTHORHOMBIC_ S	alpha-S	oF128	Fddd	A16	70	(S)
P_PHASE	Cr9Mo21Ni20	oP56	Pnma		62	(CR FE NI)24(CR FE MO NI)20(MO)12
P2S5	P2S5	aP28	P-1		2	(P)2(S)5
PI_A13	Mo3Al2C	cP20	P4_1 32	A13	213	(CR)12.8(FE NI SI)7.2(N)4
PROTO_ PYROXENE	MgSiO3	oP40	Pbcn		60	(CA+2 MG+2)1(SI+4)1(O-2)3
PSEUDO_ WOLLASTONITE	CaSiO3	mS120	C2/c		15	(CA+2)1(SI+4)1(O-2)3
QUARTZ	SiO2	hP9	P3_121 / P6_ 222	*/C8	152/180	(SIO2)
R_PHASE	Co5Cr2Mo3	hR53	R-3h		148	(CO CR FE MN NI)27(MO W)14(CO CR FE MN MO NI W)12
RANKINITE	Ca3O7Si2?	m*4	P121/a1		14	(CA+2)3(SI+4)2(O-2)7
RED_P	*	*	*			(P)
RHODONITE	MgSiO3	mP40	P2_1/c		14	(MN+2)1(SI+4)1(O-2)3
RU1S2	FeS2	cP12	Pa-3		205	(RU)1(S)2
RU2SI_C37	Co2Si	oP12	Pnma	C37	62	(RU)2(SI)1
RU2SI3	Ge3Ru2	oP40	Pbcn		60	(RU)2(SI)3

Name	Prototype	Pearson	Spacegroup	Strukturbericht	SG#	CEF Fomula unit
RU4SI3	Ru4Si3	oP28	Pnma		62	(RU)4(SI)3
RUSI	FeSi	cP8	P2_13	B20	198	(RU)1(SI)1
RUTILE_MO2	TiO2	tP6	P4_2/mnm	C4	136	(MN+4 NB+4 TI+4)1(O-2)2
S2ZR1	CdI2	hP3	P-3m1		164	(S2ZR)
SAPPHIRINE	CaMg3Si3O10	aP68	P-1		2	(AL18MG7O40SI3)
SI2Y_C32	AlB2	hP3	P6/mmm	C32	191	(Y)1(SI)2
SI2Y_CC	Si2Th	tI12	I4_1/amd	CC	141	(Y)1(SI)2
SI3N4	Si3N4	hP28/hP14	P31c/P6_3		159/173	(SI)3(N)4
SI4Y5	Gd5Si4	oP36	Pnma		62	(Y)5(SI)4
SI5Y3_C32	AlB2	hP3	P6/mmm	C32	191	(Y)3(SI)5
SI5Y3_CC	Si2Th	tI12	I4_1/amd	CC	141	(Y)3(SI)5
SIC_B3	ZnS	cF8	Fd-3m	B3	227	(SI)1(C)1
SIGMA_D8B	CrFe	tP30	P4_2/mnm	DB8	136	(AL CO CR FE MN NI RU TA V)10(CR MO NB TA TI V W)4(AL CO CR FE MN MO NB NI RU SI TA TI V W)16
SILLIMANITE	Al2(SiO4)O-a	oP32	Pnma		62	(AL+3)1(AL+3)1(SI+4)1(O-2)5
SIP1	SiP	oC48	Cmc2_1		36	(P)1(SI)1
SIP2	GeAs2/FeS2	oP24/cP12	Pbam/Pa-3		55/205	(P)2(SI)1
SIS2_C42	SiS2	oI12	Ibam	C42	72	(SIS2)
SIY_B33	CrB	oC8	Cmcm	B33	63	(Y)1(SI)1
SPINEL	Al2MgO4	cF56	Fd-3m	H11	227	(AL+3 CR+2 CR+3 FE+2 FE+3 MG+2 MN+2 NI+2)1(AL+3 CR+3 FE+2 FE+3 MG +2 MN+2 MN+3 MN+4 NI+2 VA)2(CR+2 FE+2 MG+2 MN+2 VA)2(O-2)4
TAN_EPS	TaN	hP6	P-62m		189	(TA)1(N)1

Name	Prototype	Pearson	Spacegroup	Strukturbericht	SG#	CEF Fomula unit
TI2N_C4	TiO2	tP6	P4_2/mnm	C4	136	(TI)2(C N)1
TI2ZN	CuZr2	tI6	I4/mmm		139	(TI)2(ZN)1
TI3O2	Ti3O2	hP5	P6/mmm		191	(TI+2)2(TI)1(O-2)2
TI3P	Ti3P	tP32	P4_2/n		86	(NB TI)3(P)1
TI4C2S2	Cr2AlC	hP8	P63/mmc		194	(TI)4(C)2(S)2
TIO_ALPHA	alpha-TiO	mS20	C2/m		12	(TI+2)1(O-2)1
TIO_B1	NaCl	cF8	Fm-3m	B1	225	(TI+2 TI+3 VA)1(TI VA)1(O-2)1
TIZN_B2	CsCl	cP2	Pm-3m	B2	221	(TI)1(ZN)1
TIZN10	Ti3Zn22	tP100	P4_2/mbc		135	(TI)1(ZN)10
TIZN15	TiZn16	oC68	Cmcm		63	(TI)1(ZN)15
TIZN2_C14	MgZn2	hP12	P6_3/mmc	C14	194	(TI)1(ZN)2
TIZN3_L12	AuCu3	cP4	Pm-3m	L12	221	(TI)1(ZN)3
TIZN5	*	structure unknown				(TI)1(ZN)5
TRIDYMITE	SiO2	mS144	Cc		9	(SIO2)
V4ZN5	V4Zn5	tI18	I4/mmm		139	(V)4(ZN)5
WHITE_P	*	*	*			(P)
WOLLASTONITE	CaSiO3	aP30	Å-1		2	(CA+2 FE+2 MG+2)1(SI+4)1(O-2)3
WP2	MoP2	oS12	Cmc21		36	(W)1(P)2
VZN3_L12	AuCu3	cP4	Pm-3m	L12	221	(V)0.25(ZN)0.75
X_R2O3	Nd2O3	cI26	Im-3m		229	(CE+3 CE+2)2(O-2 VA)3
Y13ZN58	Y13Zn58	hP146	P6_3/mmc		194	(Y)0.18(ZN)0.82
Y15C19_ALPHA	alpha-Y15C19	oP18	Pbam		55	(C)19(Y)15

Name	Prototype	Pearson	Spacegroup	Strukturbericht	SG#	CEF Fomula unit
Y15C19_BETA			structure unknown			(C)19(Y)15
Y2C3_ALPHA	Sc3C4	tP70	P4/mnc		128	(Y)2(C)2(C VA)1
Y2C3_BETA			structure unknown			(Y)2(C)2(C VA)1
Y2CU2O5	Cu2Ho2O5	oP36	Pna2_1		33	(Y+3)2(CU+2)2(O-2)5
Y2S2A_Y2SI2O7	La4Ge3(GeO4)O10	aP44	P-1		2	(Y+3)1(Y+3)1(SI2O7-6)1
Y2S2B_Y2SI2O7	Y2Si2O7	oP44	Pnma		62	(Y+3)1(Y+3)1(SI2O7-6)1
Y2S2D_Y2SI2O7	Ce2Si2O7	mP44	P2_1/c		14	(Y+3)1(Y+3)1(SI2O7-6)1
Y2S2G_Y2SI2O7	Y2(Si2O7)	mP22	P2_1/c		14	(Y+3)1(Y+3)1(SI2O7-6)1
Y2SIO5	Y2SiO5	mS64	C2/c		15	(Y+3)1(Y+3)1(SIO4-4)1(O-2)1
Y2ZN17	Ni17Th2	hP38	P6_3/mmc		194	(Y)0.11(ZN)0.89
Y3ZN11	Al11La3	oI28	Immm		71	(Y)0.21(ZN)0.79
YAG	Al2Ca3Si3O12	cI160	Ia-3d		230	(AL+3 CR+3 FE+3)5(Y+3)3(O-2)12
YAM	Al2Y4O9	mP60	P2_1/c		14	(AL+3 SI+4)2(Y+3)4(O-2 VA)1(O-2)9
YAP	AlYO3	hP10	P6_3/mmc		194	(AL+3 CR+3 FE+3)1(Y+3)1(O-2)3
YB12_D2F	UB12	cF52	Fm3m	D2F	225	(B)12(Y)1
YB4_D1E	UB4	tP20	P4/mbm	D1E	127	(Y)1(B)4
YB66	YB66	cF1936	Fm-3c		226	(Y)1(B)66
YC_B1	NaCl	cF8	Fm-3m	B1	225	(Y)1(C C2 VA)1
YC2_C11A	CaC2	tI6	I4/mmm	C11A	139	(C2Y1)
YCUO2	AgFeO2	hP8	P6_3/mmc		194	(Y+3)1(CU+1)1(O-2)2
YFE2O4	E(Eu0.5Yb0.5)Fe2O4	hR21	R-3m		166	(FE+2 FE+3)2(Y+3)1(O-2)4

Name	Prototype	Pearson	Spacegroup	Strukturbericht	SG#	CEF Fomula unit
YZN_B2	CsCl	cP2	Pm-3m	B2	221	(Y)0.5(ZN)0.5
YZN12_D2B	Mn12Th	tI26	I4/mmm	D2B	139	(Y)0.08(ZN)0.92
YZN3	YZn3	oP16	Pnma		62	(Y)0.25(ZN)0.75
YZN5	ErZn5	hP36	P6_3/mmc		194	(Y)0.17(ZN)0.83
Z_PHASE	CrNbN	tP6	P4/nmm		129	(CR FE)1(MO NB V)1(N VA)1
ZINCBLENDE_B3	ZnS	cF8	F-43m	B3	216	(AL)1(P)1
ZN22ZR	Zn22Zr	cF184	Fd-3m		227	(ZN)0.96(ZR)0.04
ZN2ZR_C15	Cu2Mg	cF24	Fd-3m	C15	227	(ZN)0.67(ZR)0.33
ZN2ZR3	Zr3Al2	tP20	P4_2/mnm		136	(ZN)0.4(ZR)0.6
ZN39ZR5	Zn39Zr5	mC88	C2/m		12	(ZN)0.89(ZR)0.11
ZN3P2	Mn2O3/Zn3P2	cI80/tP40	Ia-3/P4_2/nmc	D5_3/D5_9	206/137	(ZN)3(P)2
ZN3ZR_D023	Al3Zr	tI16	I4/mmm	D023	139	(ZN)0.75(ZR)0.25
ZN3ZR_HT	*	c**	*			(ZN)0.75(ZR)0.25
ZNP2	ZnP2/ZnAs2	tP24/mP24	P4_12_12/P2_1/c		92/14	(ZN)1(P)2
ZNS_B3	ZnS 3C	cF8	F-43m	B3	216	(ZN)1(S)1
ZNS_B4	ZnS 2H	hP4	P6_3mc	B4	186	(ZN)1(S)1
ZNZR_B2	CsCl	cP2	Pm-3m	B2	221	(ZN)0.5(ZR)0.5
ZNZR2	CuZr2	tI6	I4/mmm		139	(ZN)0.33(ZR)0.67
ZR2S3	Zr0.77S	mS32	C2/m		12	(S3ZR2)
ZR3Y4O12	Y6UO12	hR57	R-3		148	(ZR+4)3(Y+3)4(O-2)12
ZRO2_C43	Zro2-m	mP12	P2_1/c	C43	14	(Y+3 ZR+4)2(O-2 VA)4
ZRO2_TETR	HgI2	tP6	P4_2/nmc		137	(MN+2 MN+3 NI+2 Y+3 ZR+4)2(O-2 VA)4